

15. SITE 225

The Shipboard Scientific Party¹

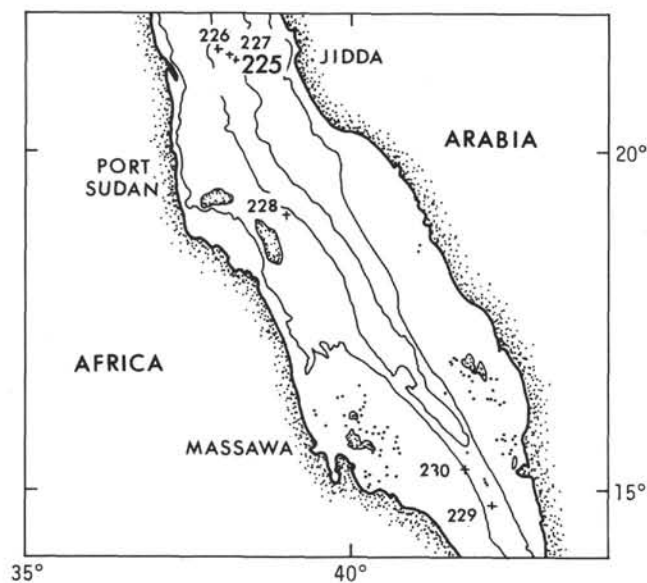


Figure 1. Bathymetric chart showing the position of Site 225 and other Leg 23 sites in the Red Sea. Contours at 500 and 1000 fathoms from Laughton (1970);

SITE DATA

Dates: 0502 15 Apr–0017 17 Apr 72

Time: 43 hours

Position (Figure 1): 21°18.58'N, 38°15.11'E

Holes Drilled: 1

Water Depth by Echo-Sounder: 1228 corr. meters

Total Penetration: 230 meters

Total Core Recovered: 137.5 meters from 29 cores

Age of Oldest Sediment: Late Miocene

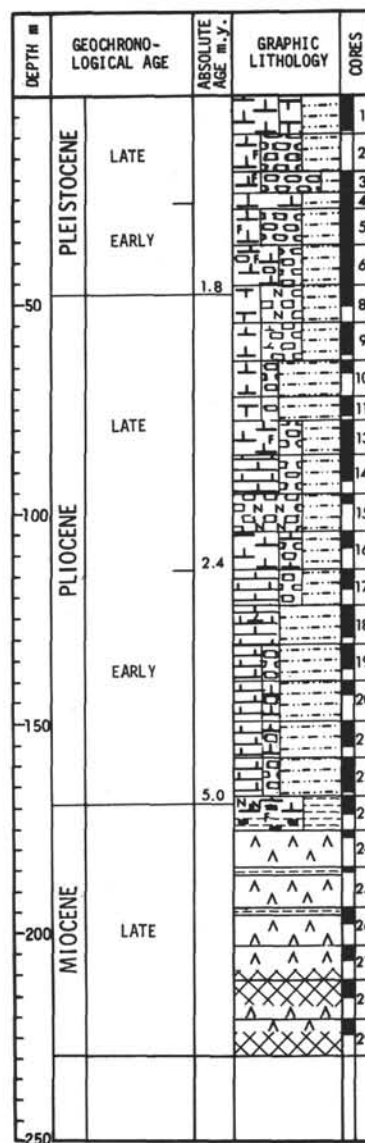
Basement: Igneous basement not reached

ABSTRACT

Site 225 was drilled on the seaward edge of the main trough about 16 km east of the Atlantis II Deep. The hole was continuously cored to a depth of 230 meters and was terminated 54 meters into a Late Miocene evaporite sequence. A distinct acoustic reflector, reflector S, mapped over much of the Red Sea, is due to the lithologic change from an overlying Early Pliocene claystone to an anhydrite marking the top of the evaporite sequence.

Lithologic and paleontologic evidence indicates that shallow restricted evaporite conditions prevailed in the Miocene, gradually changing to more open sea conditions in the Pliocene and Pleistocene.

SITE 225



¹Robert B. Whitmarsh, National Institute of Oceanography, Wormley, Godalming, Surrey, United Kingdom; David A. Ross, Woods Hole Oceanographic Institution, Woods Hole, Massachusetts; Syed Ali, State University of New York, Stony Brook, New York; Joseph E. Boudreaux, Texaco, Inc., New Orleans, Louisiana; Robert Coleman, U. S. Geological Survey, Menlo Park, California; Robert L. Fleisher, University of Southern California, Los Angeles, California; Ronald W. Girdler, The University, Newcastle-upon-Tyne, United Kingdom; Frank T. Manheim, U. S. Geological Survey, Woods Hole, Massachusetts; Albert Matter, Geologisches Institut, Universität, Bern, Switzerland; Catherine Nigrini, Lexington, Massachusetts; Peter Stoffers, Laboratorium für Sedimentforschung, Universität Heidelberg, Heidelberg, Germany; Peter R. Supko, Scripps Institution of Oceanography, La Jolla, California

Dark muds and shales above the evaporite sequence are occasionally enriched with iron, vanadium, and molybdenum. Within the evaporite sequence, shales contained smaller vanadium and molybdenum contents but considerable copper.

Interstitial salinities increase with depth and form a typical diffusion curve characteristic of saturated sodium chloride. This phenomenon, similar to that observed in several other Red Sea sites, indicates the presence of halite at depth (see Site Summary).

BACKGROUND AND OBJECTIVES

The Red Sea is of considerable importance in the recent concepts of sea-floor spreading. Physiographically, the Red Sea consists of a large main trough between the coastal shelves of Saudi Arabia and Yemen on the east and Egypt, Sudan, and Ethiopia on the west (Allan, 1966; Laughton, 1970). The main trough is best developed in the southern and central portions of the sea and usually contains a deeper intensely deformed axial trough (Figure 2). In some areas the axial trough is displaced due to fracture zones or is topographically indistinct. The latter is especially true in the southern part of the Red Sea.

Geophysical data indicate that the axial trough is underlain by oceanic crust (basalt); the composition of the material underlying the marginal zone is probably both basaltic and continental (granite?). Magnetic anomalies from the axial trough and parts of the main trough have been interpreted in terms of sea-floor spreading (Vine, 1966). The spreading rate for about the last 3 m.y. has been about 1 cm/year. High heat flow (Erickson and Simmons, 1969; Girdler, 1970) and seismicity (Fairhead and Girdler, 1970) are common in the axial trough. Seismic profiles generally indicate mildly deformed and uniformly thick postevaporitic sediment layers in the marginal zones with highly disturbed structure and generally little sediment in the axial trough (Phillips and Ross, 1970). A distinct seismic reflector (S) has been mapped over most of the Red Sea (Knott et al., 1966; Ross et al., 1969; Phillips and Ross, 1970) and is observed at depths up to 500 meters beneath the main trough, but is absent from the axial trough. This

reflector was thought to represent an unconformity of late Miocene to early Pliocene age.

Three small pools containing hot salty water have been found within a small area (around 21°N) of the axial trough (Degens and Ross, 1969). Sediments underlying the brines are enriched in a number of heavy metals, such as copper, lead, zinc, silver, and gold and may be of economic importance (Bischoff and Manheim, 1969).

Site 225 is situated on the seaward edge of the marginal zone. The site is near the brine area, but sufficiently far from the axial trough so that a substantial sedimentary section could be obtained. About 0.20 sec (about 200 m) of acoustically transparent sediments overlie reflector S, some weaker reflections occur below to a depth of 0.45 sec. A sonobuoy station taken on *Chain* cruise 100 (Ross and Schlee, in press) shows 0.15 km of material having a velocity of 1.55 km/sec (unconsolidated sediments) overlying an unknown thickness of material having a velocity of 4.5 km/sec (evaporites?).

The main objectives of drilling at Site 225 were:

- 1) Determine from the sedimentary record past connections of the Red Sea with the Mediterranean and Arabian seas.
- 2) Sample and date reflector S.
- 3) Determine the chronology and composition of the evaporite deposits and their relationship to sea-floor spreading.
- 4) Determine if there has been any effects of the nearby brines, during their migration, on the surrounding rocks.
- 5) Discover if ancient brine deposits are to be found at this locality, which may have once been part of the axial trough.

The JOIDES Advisory Panel on Pollution Prevention and Safety made several recommendations for the Red Sea drilling; the most important ones were to core continuously and to monitor downhole temperature.

OPERATIONS

Site 225 was approached on 15 Apr 72 after almost 3 days of steaming from Djibouti. Before heading for the site, *Glomar Challenger* was diverted via the hot brine area so

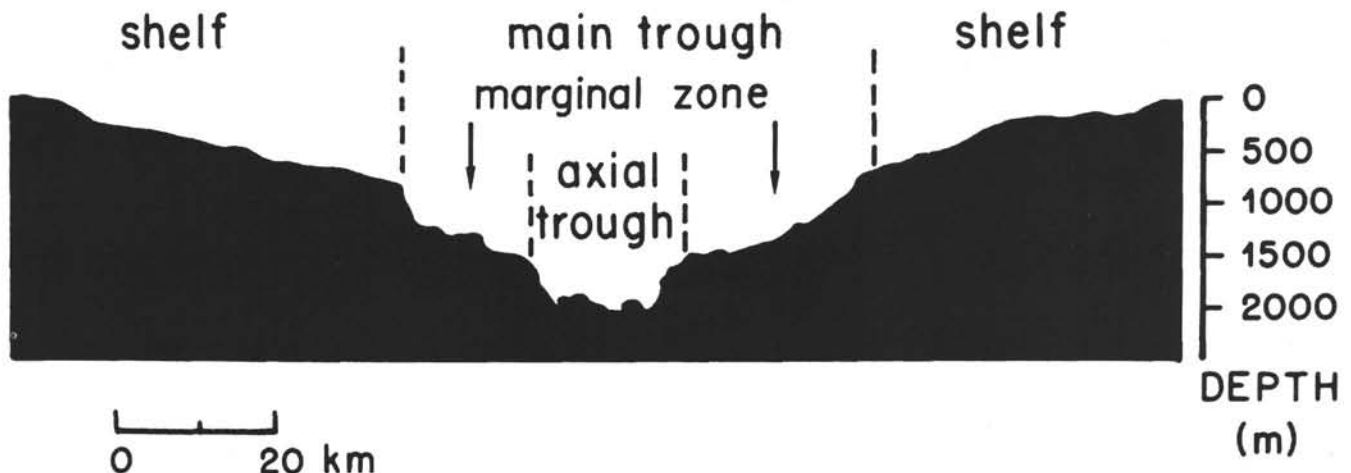


Figure 2. Main physiographic provinces of the Red Sea.

that Site 225 could be located relative to the eastern edge of the axial trough of the Red Sea (Figure 3). Atlantis II Deep was located without difficulty with the aid of satellite fixes, which also indicated a northerly current of about 1 knot during the approach to the brine pools. After traversing part of Atlantis II Deep, *Glomar Challenger* turned east-southeast at 8 knots to locate Site 225. Some time was spent on various courses looking for a site near to which the S reflector had both a smooth and a rough appearance. Such a dual nature had occasionally been seen before on sparker records and suggested the possibility of a hard sedimentary reflector lapping onto a rough (volcanic?) basement. Eventually, a site was found near to which such a relationship was discerned. A 16-kHz beacon was dropped at 8 knots at 1045 hours. Some trouble was then experienced with one of the ship's hull-mounted hydrophones which had to be repaired before the ship could hold station over the beacon. A complicating factor during the presite survey was the lack of satellite fixes for the 4 hours before dropping the beacon and the presence of an unexpected 1 knot easterly current.

No problems were encountered during the drilling operations at this site. Coring, at the request of the Safety Committee, was done continuously. For the 230-meter cored interval, we recovered 137.5 meters of core (60%). The first seven cores, in an Upper Pleistocene mud with occasional lithic fragments, were easily penetrated and drilling time per core averaged about 15 minutes (Table 1). Cores 3, 7, and 12 were unintentionally obtained while using the Von Herzen temperature probe.

After Cores 6, 16, and 28, a new bottom hole water sampler was tested. This device, a modification of the Kuster Formation Sampler, takes a sample of fluid at the bottom of the hole, retaining the original pressure until the

tool is opened at the surface. In the first test, comparison of bottom fluid salinity with interstitial water salinity (squeezed from cores) on one hand, and surface water (drilling fluid) on the other, showed that the bottom fluid consisted of about 81% surface water and 19% true formation fluid. Low gas levels were noted.

Cores 8 to 23 were taken in Pliocene carbonate ooze. Cutting time was generally about 20 minutes, with a bit weight of 5-10,000 lb for Core 11, then 10-12,000 lb for Core 22, and 15-20,000 lb for Core 23. Cores 17 and 18 had gas shows, but chromatography showed it to be mainly air. Interstitial water salinities were 64‰, 95‰, and 136‰ for Cores 18, 21, and 23, respectively. The increasing gradient suggested salt below.

From Core 24 to the final core, 29, a fairly resistant evaporite sequence was encountered. Drilling time averaged about 1 hour per core, reaching a maximum of 85 minutes for Core 26, which was composed mainly of anhydrite. Bit weight was 15-20,000 lb for Cores 24 and 25, and 20-22,000 lb for Cores 25 to 29.

All geological objectives were achieved, and we decided to abandon the hole after Core 29 was pulled at a total depth of 230 meters. The hole was filled with mud.

The ship departed from the site at 0317 hr 17 Apr 72. An easterly course was maintained while the seismic profiling gear was streamed. The ship then turned to port onto a course of 280° and passed within 1000 feet of the sea-bed beacon. This course was maintained as far as the next site in Atlantis II Deep.

LITHOLOGY

At Site 225 a 230-meter-thick stratigraphic section was continuously cored. Table 2 shows the major lithologic units and their approximate depths and thicknesses.

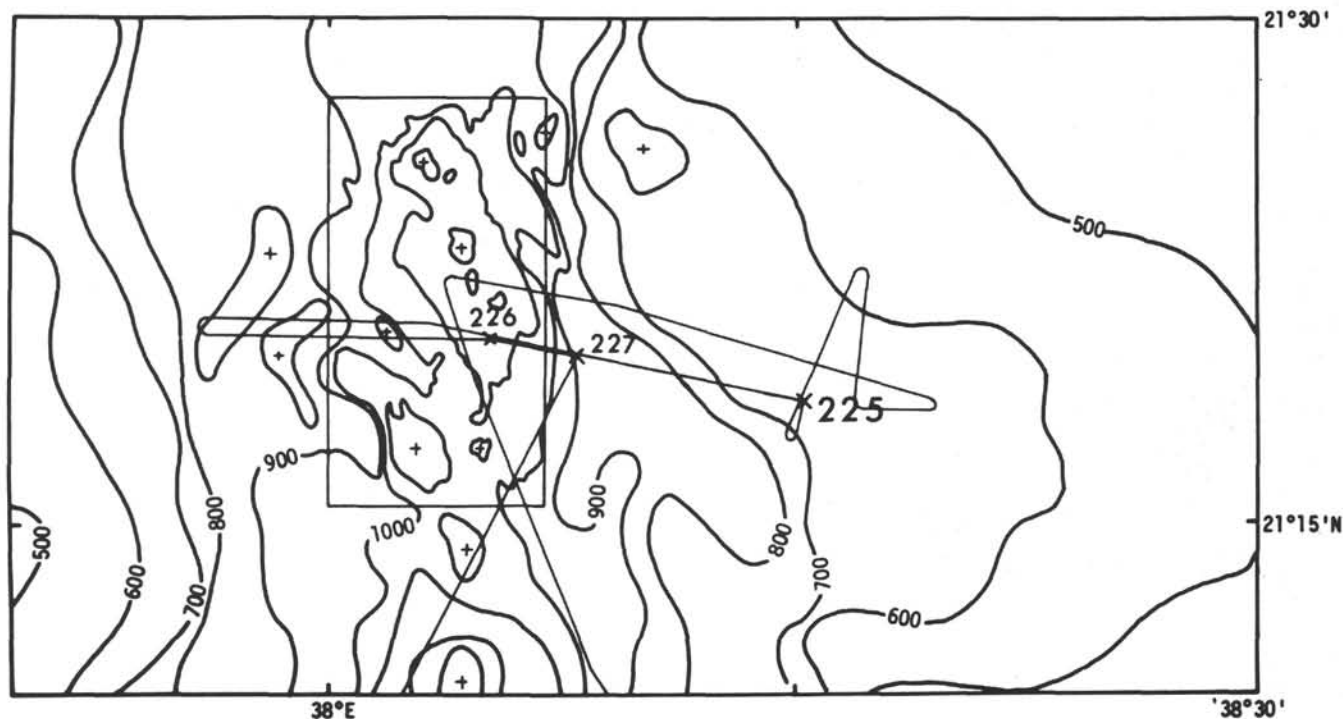


Figure 3. Bathymetric chart of the area around Sites 225, 226, and 227 with the tracks of *Glomar Challenger*. Contour interval 100 fathoms, depths in corrected fathoms. Contours within box from Amann (1972), other contours based on collected soundings too numerous to show clearly (after Laughton, unpublished).

TABLE 1
Coring Summary, Site 225

Core	Date/Time Core on Deck (Time Zone-3)	Subbottom (m)	Cored (m)	Recovered (m)
1	15 Apr: 1250	0-9	9.0	9.3
2	1330	9-18	9.0	0.0
3 ^a	1415	18-23	5.0	5.0
4	1452	23-27	4.0	8.4
5 ^b	1545	27-36	9.0	8.0
6 ^b	1625	36-45	9.0	9.3
		42 ^c		
7 ^a	1805	45	0.0	0.0
8 ^b	1845	45-54	9.0	4.5
9 ^b	1925	54-63	9.0	8.3
10 ^d	2015	63-72	9.0	2.3
11 ^b	2055	72-77	5.0	7.6
12 ^a	2150	77	0.0	1.0
13	2235	77-86	9.0	8.7
14	2325	86-95	9.0	5.5
15	16 Apr: 0010	95-104	9.0	2.2
16	0110	104-113	9.0	3.3
-		110 ^c		
17	0220	113-122	9.0	5.0
18	0310	122-131	9.0	7.5
19	0415	131-140	9.0	6.0
20	0510	140-149	9.0	2.5
21	0615	149-158	9.0	4.1
22	0715	158-167	9.0	9.0
23	0807	167-176	9.0	4.5
24	0955	176-185	9.0	1.5
25	1135	185-194	9.0	0.9
26	1335	194-203	9.0	3.0
27	1520	203-212	9.0	3.0
28	1635	212-221	9.0	3.8
-	1725	218 ^c		
29	1910	221-230	9.0	3.3
-	2010	227 ^e		
		Total	230.0	137.5

^aHF = Von Herzen temperature probe run.

^bCirculation broken.

^cFluid sampler.

^dSpotted mud after Core 10.

^eRecording thermometer

Unit I

This unit consists of soft to semilithified light to dark gray foram-bearing, micarb-rich detrital clayey silt nanno ooze and chalk. These oozes and chalks are mainly composed of nannofossils 30-50%, carbonate particles (micarb) 10-30%, foraminifera 5-10%, and detrital silt and clay 30-60%. Minor amounts of pyrite and volcanic glass occur throughout this unit (see Site Summary).

The sediments of unit I display a variety of colors—light brown, light gray, greenish gray, dark gray, and black—separated by fairly sharp color boundaries. These colors are believed to reflect the Eh of the sediments at the time of their deposition; a brownish color indicating oxidizing conditions, greenish gray and black indicating reducing conditions. The dark layers are enriched in organic matter and pyrite. Smear slide examination reveals that in the dark layers, nannofossils and foraminifera are diagenetically less recrystallized than in the lighter color sediments.

Bedding characteristics of unit I are variable. Beds (1-2 cm thick) are only visible in zones with higher silt and clay content. Most of the sediments of unit I are lightly to moderately burrowed, the burrowing being generally more common in light-colored chalks.

Nannofossil content is apparently uniform throughout this unit. Planktonic forams are abundant in the upper 100 meters and benthonic forams, which are probably indicative of upper bathyal and neritic water depths, occur only in the lower 100 meters of the unit.

In Cores 1 through 8 broken pieces of lithified carbonate occur.

Unit II

This unit consists of gray semilithified to lithified micarb nanno detrital silty claystone (composition: nannofossils 20-40%, micarb 5-15%, detrital silt and clay 20-60%). Unit II differs from unit I in having a high terrigenous component. Similar to unit I, there are alternating light gray and dark gray layers. The dark gray layers are enriched in organic matter and pyrite. Most of the sediments in this unit are slightly to moderately bioturbated.

Unit III

This unit is characterized by dark gray to black semilithified dolomitic silty claystone (composition: detrital silt and clay 20-70%, dolomite 20-60%, pyrite 5-15%). Analcite is a common constituent of the clays.

TABLE 2
Lithologic Summary, Site 225

Lithologic Units	Thickness (m)	Subbottom Depth (m)	Core
I Gray FORAM-BEARING MICARB RICH DETRITAL CLAYEY SILT NANNO OOZE and CHALK	112	0-112	1-17
II Gray MICARB-RICH NANNO DETRITAL SILTY CLAYSTONE	55	112-167	18-22
III Dark Gray DOLOMITIC SILTY CLAYSTONE	9	167-176	23
IV EVAPORITES	>54	176-	24-29

Some parts of the unit show a slight lamination. Smear slide examination of some of the dark layers shows the abundance of pyrite and millerite.

Unit IV

Lithified anhydrite and halite characterize unit IV. The anhydrite is laminated to nodular. The evaporite facies contain several black shale layers. These very finely laminated shales are composed of clay, organic matter, and pyrite. Although a time constraint only allowed the recovery of about 54 meters of anhydrite and halite at this site, it is estimated, from seismic reflection information from the southern Red Sea, that up to 5 km of bedded evaporites is possible (Lowell and Genik, 1972).

A detailed description of this unit together with a discussion of its origin are given by Stoffers and Kühn (this volume).

Due to limited space, the tables of grain size, carbon carbonate, and X-ray data are presented with the data of the other sites in Appendices I, II, and III, respectively, at the end of the volume.

BIOSTRATIGRAPHY

Foraminifera

At no horizon, at this or any other site in the Red Sea, are planktonic foraminifera sufficiently diverse or diagnostic to permit the recognition of zones which can be conclusively correlated directly with evolutionary foraminiferal sequences in open-ocean, deep-sea sediments. Ecological control of the species composition of Red Sea faunas has been severe during the late Neogene, and very few faunal events which have time-significance outside the Red Sea were observed. The contrast of these restricted faunas with the well-developed nannofossil floras is striking.

It is possible, however, to divide the observed faunas into three main planktonic biofacies. The first of these, which will be termed the "*Globigerinoides sacculifer* Biofacies," is similar in species composition to the assemblages reported by Berggren and Boersma (1969) in their Zones A and D. The planktonic populations are relatively diverse, by Red Sea standards, and may contain as many as a dozen species; the most abundant, generally, are *Globigerinoides quadrilobatus sacculifer*, *G. ruber*, *Globigerinella siphonifera*, and *Orbulina universa*. Berggren and Boersma did not examine the smaller size fractions in detail; among these forms, *Globigerinita glutinata* and *Turborotalita quinqueloba* are quite abundant. In many samples, these populations are somewhat restricted, and the relatively common occurrence of *G. quadrilobatus sacculifer* was generally used as a basis for assigning an assemblage to this biofacies.

The second group, the "*Globigerinoides ruber* Biofacies," includes populations whose larger fractions are almost entirely dominated by *G. ruber*, with *G. quadrilobatus sacculifer* virtually absent. In Pliocene sediments, *G. obliquus obliquus* and *G. obliquus extremus* are usually associated with *G. ruber*, and *Globigerinita glutinata* and *T. quinqueloba* are usually common.

In the "*Globigerinita glutinata* Biofacies," the common species are *G. glutinata* and *T. quinqueloba*, although in

*"This chapter will now be published in Volume 24 of the Initial Reports series."

some samples only the latter is present. Larger species are very rare or absent. In a few samples, *Globigerina bulloides* or *Turborotalia* sp. may be present in this assemblage.

Benthic foraminifera, while usually present, are generally not common, except in Lower Pliocene sediments. Two general faunal associations, with different species compositions, are present, one approximately associated with the Pleistocene and the other with the Pliocene. The benthic faunas are discussed in greater detail in the chapter on Red Sea foraminifera (Fleisher, this volume*), but none of the species observed is characteristic of environments deeper than neritic to upper bathyal.

At Site 225, the *Globigerinoides sacculifer* Biofacies is dominant from Core 1 to Sample 9-5, 58-60 cm, although at some horizons, particularly in Cores 4, 5, and 9, *G. ruber* is much the dominant species. The *G. ruber* Biofacies is present from Samples 9-6, 46-48 cm to 13, CC; the highest occurrence of *Globigerinoides obliquus* is in Sample 10-1, 112-114 cm. Cores 14 and 15 contain assemblages of the *Globigerinita glutinata* Biofacies, as well as the highest occurrence of the Pliocene benthic suite.

No consistent patterns could be recognized in Cores 16 through 20; faunas in these cores fluctuate irregularly between the *G. ruber* and *G. glutinata* Biofacies. Planktonic species are very rare or absent in Core 21 through Sample 22-2, 50-52 cm. *Turborotalita quinqueloba* is common in the remainder of Core 22, but planktonics are essentially absent below this core. Benthic foraminifera are present as low as Core 24, but absent below.

Nannofossils

A complete Pleistocene and Pliocene stratigraphic section is present at this site.

The *Gephyrocapsa oceanica* Zone (Boudreaux and Hay, 1969) is very well represented with abundant nannofossils of the Late Pleistocene in Sample 1-3, 65-66 cm. *Gephyrocapsa caribbeanica* appears in Sample 1, CC. The *Coccolithus dornicoides* Zone of Late Pleistocene is present in Core 3. *Gephyrocapsa caribbeanica* (Boudreaux and Hay, 1969) also occurs abundantly in the *C. dornicoides* Zone. The *Pseudoemiliana lacunosa* Zone appears in Sample 4-5, 130-131 cm.

Samples 8-6, 134-135 cm and 8, CC contain elements of the *Discoaster brouweri* Zone of Late Pliocene. *Pseudoemiliana lacunosa* is also present at this level. The *Discoaster brouweri* Zone extends from Core 8 through Core 9. The *Discoaster pentaradiatus* Zone is well represented in Cores 9 and 10, and the *Discoaster surculus* Zone occurs in Cores 11 through 14. Abundant *Sphenolithus abies* are present in Cores 15 and 16. The extinction level of *Reticulofenestra pseudoumbilica* is present in Core 17 and represents the top of the Early Pliocene. The *Reticulofenestra pseudoumbilica* Zone extends from Core 17 through Core 20. *Ceratolithus tricorniculatus* is present in Cores 20 and 21. The *Discoaster asymmetricus* Zone is present in Sample 22, CC.

Core 23, Section 2 contains common occurrences of *Discoaster quinqueramus* of Late Miocene. Nannofossils are completely absent from the evaporite sediments encountered in Cores 25 through 29. The Late Miocene Zone of *D. quinqueramus* in Core 23 is the last reliable geological age

and was obtained in the black sediments overlying the evaporite sequence of anhydrite and salt found in Cores 24, 25, 26, 27, 28, and 29.

Radiolaria

Above Core 19 siliceous microfossils are absent from Site 225 material. In Sample 19-4, 101-103 cm rare, pyritized Radiolaria, diatoms, and silicoflagellates were observed; preservation is poor with the radiolarians and diatoms present only as fragments. In the core catcher of Core 19 and in Core 20, Section 1 there are a few radiolarians which have been recrystallized to analcite. They show a good birefringence and minimal structure. In Sample 25-1, 83-85 cm a few, moderately well preserved diatoms and a single fish tooth are present. No age determination was made on these forms.

Palynology

Samples 28-2, 68-72 cm and 29-3, 39-42 cm from with the evaporite sequence were examined for spores and pollen by Dr. David Wall of the Woods Hole Oceanographic Institution, but none were found.

Biostratigraphic Summary

Nannofossils are abundant at Site 225 in sediments deposited in open marine environments of the Red Sea. Floral assemblages in the Pleistocene sediments greatly resemble those found in carbonate environments of the Caribbean Sea, and all of the world-wide Late Miocene to Late Pleistocene index species are present. Nannofossils are very rare or completely absent from the evaporite section encountered at this site.

Planktonic foraminifera are the dominant faunal element in the upper 130 meters of recovered sediment and are rare to absent below. Planktonic assemblages, however, are nondiverse, generally consisting of only four or five species, and are not diagnostic for purposes of age determination. Upper bathyal and neritic benthonic foraminifera first appear in abundance in Core 10 (72 m below sea floor), and while the faunal relationships are unclear, they seem to indicate slight shallowing by Core 21. Below this level, they are present only within Core 24, Section 1.

Badly preserved Radiolaria are found in sediments recovered in Cores 19 and 20. Moderately well preserved diatoms are present in Sample 25-1, 83-85 cm.

Investigations suggest that a complete stratigraphic section exists in the Pleistocene and Pliocene of Site 225. A well-lithified interval rich in inorganic carbonate and almost devoid of nannofossils is present at the base of Core 7, which is suggestive of a eustatic drop in sea level related to an Early Pleistocene glacial stage. Further studies of the Pleistocene section may reveal other evidence for glacial stages in the younger sediments.

Evaporites consisting of anhydrite and salt were encountered in Cores 24 through 29 and are present below the Late Miocene extinction level of *Discoaster quinqueramus* (Bukry, 1971), which is present in Core 23. The absolute age assigned to sediments encountered in the *D. quinqueramus* Zone in this core is 5.0 million years.

Sedimentation Rates

Sedimentation at this site (Figure 4) was slowest during the Late Miocene and Early Pliocene interval (150-180 m), after the termination of evaporite deposition. During the late Early Pliocene, the sedimentation rate gradually increased from 20 m/m.y. to the much higher Late Pliocene (50-110 m) value of 100 m/m.y. Although samples containing floras representative of both the *Pseudoemiliana lacunosa* and *Discoaster brouweri* were recovered, the sedimentation curves suggest a Late Pliocene or Early Pleistocene modification in sedimentation. Whether this represents an unconformity or an abrupt change in sedimentation rate cannot be determined, as the change apparently occurs within the *P. lacunosa* Zone. The accumulation rate for Quaternary sediments decreased slightly (to 70 m/m.y.) from Late Pliocene values.

GEOCHEMISTRY

Geochemical aspects include the chemical composition of solids and interstitial waters squeezed from cores, gases, total water content, and diffusional parameters.

Solids

Site 225 sediments consisted, throughout the upper 178 meters, of carbonate muds with lithified layers and occasional bands of dark green to brown muds, becoming shales in the lower part of the hole. Below 178 meters anhydrite and halite rocks also contained some dark shaly interbeds. The upper dark muds and shales contained substantial iron, generally above 5% Fe, chiefly combined as pyrite, but also unusually large amounts of vanadium and molybdenum. As much as 500 ppm Mo and 1000 ppm V were found by the shipboard spectrographic analyses, values reached only in some of the classical "black shales" such as the Mansfelder Kupferschiefer and Swedish Alum shales. Within the lower evaporite sequence, shales contained much lower vanadium and molybdenum, but appreciable copper (200 ppm).

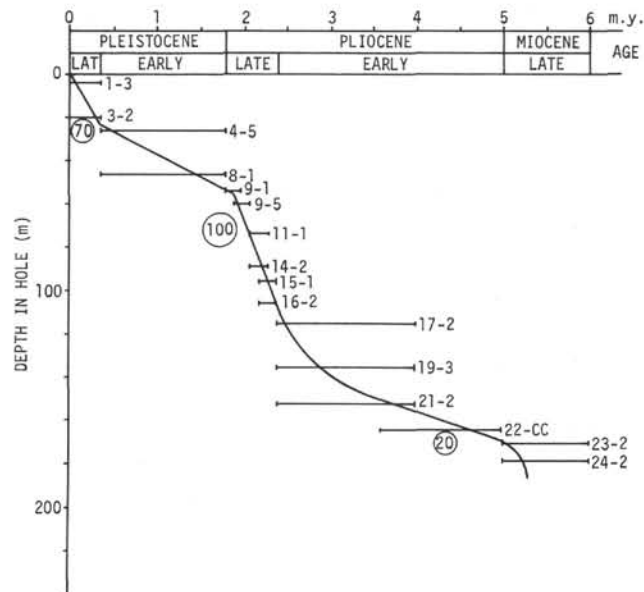


Figure 4. Sedimentation rates at Site 225. Plotted bars are those sufficient to control slopes of lines.

Selected samples of pyrite picked from the carbonate muds also contained substantial nickel (500 ppm) and 100-200 ppm copper, but no phases investigated showed appreciable lead or other heavy metals. One extraordinary pyrite sample contained 3000 ppm arsenic as well as 500 ppm antimony. It has a silvery-white sheen like that of arsenopyrite.

The carbonate muds contained high magnesium concentrations (5% Mg), reflecting appreciable high magnesian-calcite content and some dolomite. Toward the base of the section, the increasing dolomite observed by the petrologists showed itself in even higher magnesium concentrations. Several lithified fragments contained on the order of 5000 ppm strontium. This order of strontium is indicative of authigenic aragonite, which in pure form contains upwards of 8000 ppm Sr. High strontium aragonite is rare in the oceans, excepting surficial deposits; however, it has been found in Red Sea cores by Milliman et al., 1969, and the present findings extend its depth range to over 100 meters depth in the sediments (see also Stoffers and Kühn, this volume).

Manganese values average around 0.1%, typical of shelf sediment values in the Red Sea (Manheim, unpublished data). In the rift valley the values are much higher, averaging around 1%, even in nonactive (nonbrine or metal-rich) areas.

The onboard spectrograph was especially useful in being able to analyze small (as little as 0.5 mg) grains or segregates picked out under the microscope. Some clearly recrystallized, partly obliterated foram tests from the lower part of the section showed both low magnesium and low strontium, suggesting that low magnesium calcite is a stable carbonate recrystallization product at depth.

The anhydrites and rock salt are low in trace metals, as anticipated. However, of special interest is the fact that a dried sample of pore fluid from the lower part of the section showed detectable Pb, corresponding to about 1 ppm fresh brine. This shows that brines obviously unassociated with any volcanism or other thermal activity are capable of being enriched in heavy metals.

Interstitial Waters

Immediately below the sea bed small but unmistakable increases in interstitial salinity were observed. These increases, flattened out somewhat at some tens of meters depth, finally rose dramatically to form a classical diffusion curve toward values characteristic of saturated sodium chloride (Figure 5). It was clear, taking into account similar phenomena observed in other DSDP legs, that a major source of salt was present at depth, but the slope of the curve rendered it unlikely that the reflector seen at about 170 meters depth on the seismic record was rock salt. That was encountered first at 200 meters.

Careful examination of the anhydrite between 170 and 200 meters failed to confirm any appreciable admixture of halite, but the laminar and nodular anhydrites show disturbance and textures typical of salt breccias or deformations due to leaching of salt. These beds may then be remnants of much greater thicknesses of salt which have been leached away and in part reside in the higher salt content of pore waters in the overlying sedimentary rocks.

pH measurements on pore fluids showed an interesting trend from about 7.8 near the sediment-water interface, to 7.0 and below in the lowermost saline brines. We note that these brines are rather close in salinity to the brines of the hot brine deeps. Alkalinities were generally low (Table 3), but a sharp increase occurred in Core 3, coincident with the maximum (though still rather small) gas quantities found at Site 225.

One "hot squeeze" (extraction of pore fluid by means of a heated squeezer) was undertaken at the presumed bottom hole temperature, based on the thermal gradient established in the upper part of the sediment column. Results from this squeezing are discussed in Manheim et al. (Chapter 35).

Bottom Water Samples

A new tool was successfully tested at Site 225. The device is a bottom hole water sampler, modified by DSDP from the Kuster Formation Sampler. It captures a sample of fluid at the bottom of the hole, retaining original pressure until the tool is opened at the surface.

Under normal conditions bottom water will be mostly drilling fluid, but should contain any hydrocarbon gases which outgas or diffuse into the hole from surrounding rocks. Where pressures in the formation are higher than in the drilling fluid column, fluids will flow into the hole. Thus, the sampler may be a means of determining when excess pressures in bottom formations are tending to drive fluids into the well bore. This will be evident by the difference between sampled water and interstitial water squeezed from cores (internal parts). The latter have been shown to approach actual fluids in the formation (see Interstitial Water Reports in Initial Reports, Volumes 1-9). In fact, such measurements may be the only way to confirm flowing bottom waters or high pressures, since the flapper valve now prevents upward movement of well bore fluid when new joints are added to pipe.

In the current tests, the proportion of bottom fluid in Test 1 was 19%, in 2, 0%. In Test 3 it was probably very low because although bottom water was salty, the surrounding rock was anhydrite and salt, and highly impermeable (Table 4).

Gas tests in all three samplings showed extremely low hydrocarbon values, although the tester succeeded in eliminating atmospheric contamination very well. This was shown by the absence of high peaks for carbon dioxide, which otherwise characterize ambient laboratory air.

Operation of the instrument as used on Leg 23 is described under Geochemical Methods (Chapter 2).

Water Content and Consolidation

Water contents dealt with here are derived from measurements of water loss on heating. Other sediment density measurements, derived from physical measurements (e.g., GRAPE) are described in the section on Physical Properties. Water content values are listed in Table 5 and plotted in Figure 6. It should be noted that the upper parts of the section were extremely badly deformed, with admixture of a drilling "paste" or slurry. Frequently, after some exposure to air, the slightly dried split cores would show islands of "true" clumps or fragments of sediment (see Geochemical Methods, Chapter 2) which showed bedding planes and

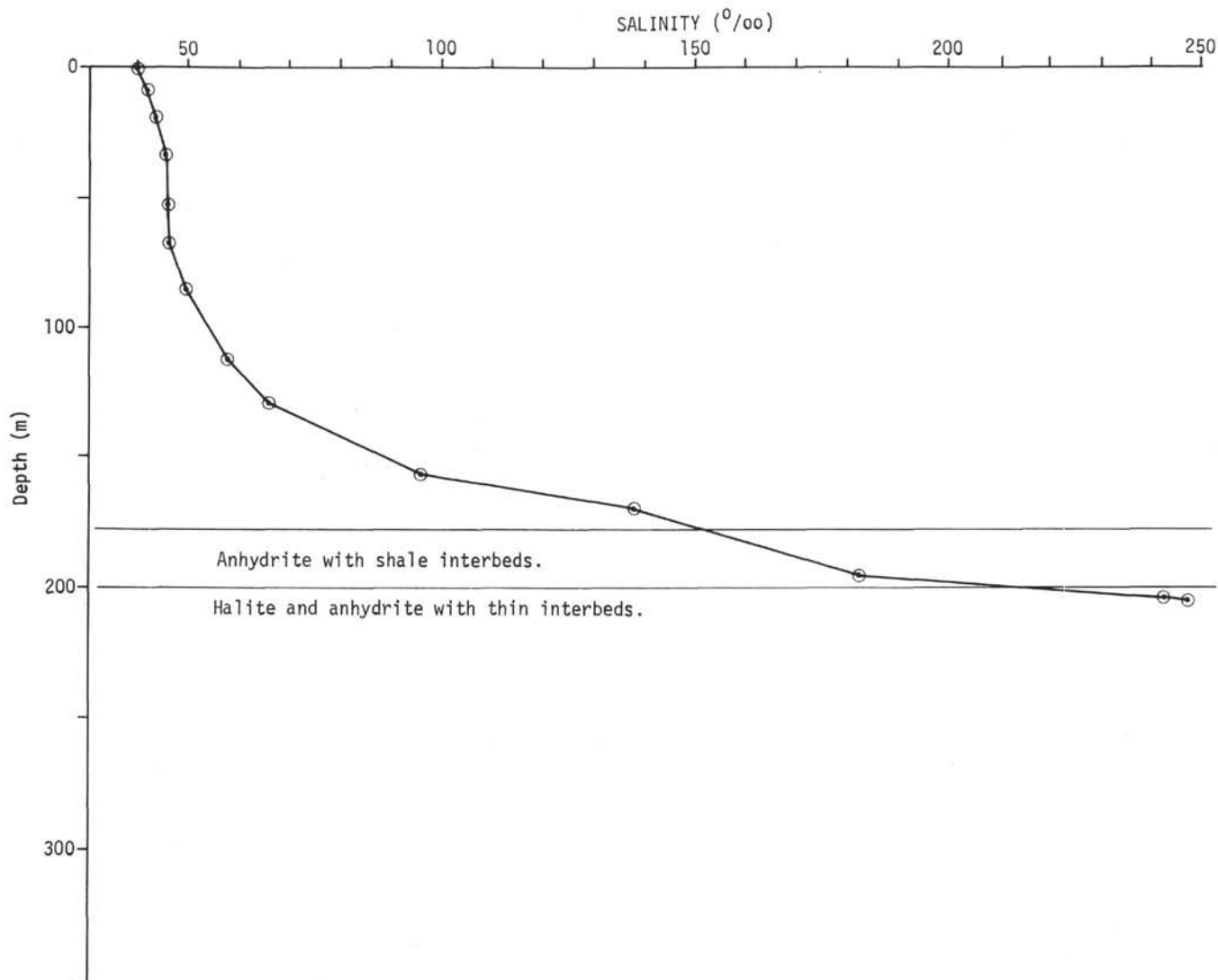


Figure 5. Interstitial salinity (g/kg) as determined by index of refraction onboard ship. Note that the "salinities" are calibrated on a seawater basis and are not to be equated with a true total dissolved solids or seawater definition (see Manheim *et al.*, chapter 35).

greater consolidation, surrounded by a mush of drilling slurry. A great effort was made to select these islands for analyses of the 1-g water content sample, at least from Core 13 downward. Arbitrary selection of syringe samples at fixed intervals is clearly an undesirable procedure, and geologist's discretion and careful poking and examining is much more preferable.

One might at first assume that the erratic zigzags on Figure 6 simply reflect sampling and deformation problems. This is not necessarily true, for recent piston cores from areas near Site 225 on R/V *Chain* cruise 100 (Manheim, unpublished data) and very careful examination of water content showed a surprisingly large variation in degree of consolidation, even for adjacent layers. Careful picking of samples in the lower parts of the site where the undisturbed nature of sections could be verified also confirmed the erratic distribution of porosity and water content.

Lithified carbonate layers of irregular and highly porous character were common and are not reflected in the water

content values, since such layers were rarely sampled. Previous studies showed that such fragments varied in water content from 10% to 30%, averaging about 20% to 25%.

A transition (in shale and carbonate consolidation) led to the very consolidated evaporite zone which began at 178 meters. Anhydrites varied in water content from 4% to less than 1%. Halite (rock salt), first encountered at 210 meters, has virtually no porosity at all. However, between the halite and anhydrite occur shale beds and shaly anhydrites, which reached 20% water content. This was fortunate for the interstitial water studies, for it enabled us to extract pore fluids even in this highly consolidated section.

Diffusimetry-Resistivity Measurements on Cores

Table 6 contains the resistivity and formation factor results for this site. For a detailed description of the techniques employed and resistivity data, see the relevant section on diffusimetry (Chapter 2).

TABLE 3
Interstitial Water Properties, Site 225

Core, Section, Interval (cm)	Subbottom Depth (m)	H ₂ O Recovered (ml)	Punch-in pH ^a (mv)	Pore Water pH	Lab Temp (°C)	ΔN	Corr Salinity (‰)	Alkalinity (meq/kg)	Sp G
Surface Seawater ^b Water ^b				8.55	26.2	70.5	39.9	—	—
1-6,0-10	9	16	2.5(25.7)	7.73	26.2	74.0	41.3	1.9	—
3-4,0-10	20	16	10.2(25.2)	7.60	26.2	78.0	43.5	4.5	—
5-6,0-10	35	17	5.3(25.3)	7.71	26.1	81.5	45.4	2.2	—
8-3,140-150 ^{b,c}	53	27	9.5(24.0)	7.76	26.4	81.5	45.4	1.7	—
10-2,0-10 ^d	67	21	—	7.56	26.4	82.5	45.9	2.3	—
13-6,0-10	86	16	—	7.54	26.8	93.5	52.0	—	—
16-3,140-150	113	11	—	7.57	26.6	103.4	58.1	1.4	—
18-4,140-150	130	10	—	7.23	25.6	117.8	65.3	—	—
21-3,0-10	157	11	—	7.02	26.2	172.0	95.2	—	—
23-2,140-150	170	6	—	7.00	25.1	247.5	136.7	(2.4)	—
26-1, 43 ^e	197	2½	—	~7.00	26.0	319.0	182	0.60	1.111
28-2 ^f	205	5	—	—	26.0	—	242	<1.0	—
28-2 ^{f,g}	(206)	3	—	—	35.0	—	246	<1.0	—

Note: Analysts: F. Manheim and D. Marsee.

^aNumber in parenthesis is temperature in core.

^bDifficult to distinguish "true" sediment from deformed paste due to disturbance in drilling and coring.

^cHighly disturbed sample.

^dSediment too stiff for punch-in pH measurement.

^eSpecific gravity by micropycnometer.

^fSalinity off scale for refractometer; diluted by weighing (Cahn Electrobalance) prior to refractometry.

^gSqueezing for 45 minutes in heated squeezer. Temperature determined by thermocouple.

TABLE 4
Bottom Water Sampler Results

Number	Depth (m)	Depth Below Seabed (m)	Salinity (‰)	Alkalinity (meq/kg)	Interstitial Salinity (‰) ^a	Surface Water Salinity
BW-1	1270	42	40.5	1.78	45.3	39.4 ^c
BW-2	1338	110	39.4	—	57.2	39.4
BW-3	1446	218	117.6 ^b	—	242.	39.4

^aBased on index of refraction. The refractive index-salinity relationship employed is that for seawater and does not apply strictly to the stronger brines.

^bBelieved due chiefly to dissolution of rock salt, rather than formation fluid admixture, since bottom formations are extremely impermeable.

^cUncorrected

Isotope Studies

Studies of the stable isotopes of oxygen and carbon have been made on pore waters and carbonates from this site by Lawrence (this volume). The deuterium/hydrogen ratio was determined from interstitial water samples by Friedman and Hardcastle (this volume). Sulfur isotope measurements were made by Shanks et al. (this volume) on anhydrite samples.

PHYSICAL PROPERTIES

Water Content, Porosity, and Density

Sediments from the top 176 meters (Pleistocene and Pliocene), described as detrital clayey silt-rich carbonate

nanno oozes and chalk, show very little systematic variation with depth. The porosity is fairly constant at about 50% and the density at about 1.8 g/cm³ (see Site Summary). The exceptions are Core 1, where the porosity reaches 77% and the density 1.4 g/cm³, and the 15 meters above the evaporites, where the porosity decreases to about 45% and the density increases to about 1.9 g/cm³. The exceptional values at the top are due to the soupy nature of the first core. It is perhaps surprising that there is no obvious systematic increase in density with depth throughout this sediment column.

At 176 meters there is a sharp change in lithology to an evaporite series (Late Miocene) consisting of anhydrite and halite with interbeds of pyrite-rich dolomitic claystone. As expected, there is a corresponding sharp decrease in water

TABLE 5
Water Content, Site 225

Core, Section, Interval (cm)	Estimated Depth (m) ^a	H ₂ O (%)	Porosity (%) ^a	Density (g/cm ³) ^a
1-1,128	1	36.9		
1-2,42	2	34.6		
1-5,45	8	34.9		
1-6,10	9	35.3		
3-1	19	28.3		
3-2	20	25.4		
3-3	22	25.2		
3-4	21	26.3		
3-4	22	27.1		
4-1	23	34.5		
4-2	23	28.3	55.4 ^b	1.96 ^b
4-3	24	37.9		
4-4	25	38.1		
4-5,85	26	55.1		
4-5,108	27	35.0		
4-6	27	40.0		
5-1	27	29.8		
		(44.6?)		
5-3,80	30	37.8		
5-4,145	32	39.7		
5-5,140	33	40.3		
5-6	35	40.9		
5-6	36	27.8		
6-1,73	37	34.8		
6-5,123	42	35.6		
6-6,113	44	39.8		
8-3,80	48	36.4		
9-3	48	25.5		
9-4,35	50	29.5		
9-5,70	51	40.7		
9-6,60	54	25.8		
10-2,90	57	27.8		
11-4	75	24.0		
12-1,110	77	41.5		
13-4,23	81	38.7		
13-4,70	82	41.8		
13-4, 120	84	41.8		
13-6,50	86	25.0		
14-1,100	87	10.3		
14-1,112	88	28.3		
14-2,127	90	33.1		
14-4,10	93	33.7		
14-4	94	31.8		
15-2,82	97	23.0		
16-2,80	106	12.8		
16-3	108	20.4		
17-2,40	115	13.3		
17-3,50	117	25.1		
17-4,130	120	12.9		
18-1,60	123	17.3		
18-2,20	127	25.1		
19-1,137	133	35.3 ^c		
19-4,23	138	35.8 ^c		
20-1,35	142	44.3		
21-3,10	153	35.1		
22-5,50	165	25.4		
23-1,139	170	15.1		

TABLE 5 – Continued

Core, Section, Interval (cm)	Estimated Depth (m) ^a	H ₂ O (%)	Porosity (%) ^a	Density (g/cm ³) ^a
24-1	179	3.6		
24-1,150	180	4.1		
26-1		(40.8) ^d		
26-1	198	<1.0 ^e		
26-1,25	199	20.7 ^f		
27-1	206	1.26		
27-1	208	0.56		
27-2,75	209	9.16		
29	225	<0.5 ^g		

Note: Values in % bulk sediment. Syringe samples in pastier sections; spatula or hammer used to break off 1-g portions in denser sections.

^aDepths usually attributed arbitrarily according to section number and cored interval, owing to impossibility of establishing exact origin.

^bBased on volume in syringe sampler.

^cAppeared to be authentic, in spite of high water content.

^dProbably erroneous.

^eDense anhydrite.

^fShale.

^gHalite rock.

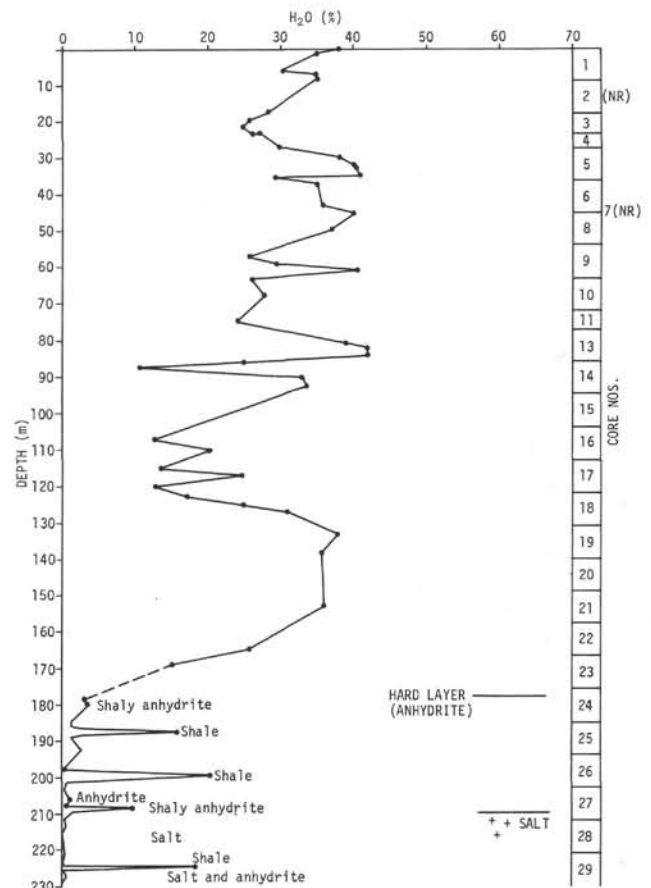


Figure 6. Water content values of sediments at Site 225.

TABLE 6
Resistivity Measurements, Site 225

Core, Section, Interval (cm)	Subbottom Depth (m)	R_s (app)	T (°C)	R_w (app)	T (°C)	R_{pw}	T (°C)	S (‰)	R_s	C	F
1-6	9	0.0910	25.1	—	—	0.168	25.6	41.3	0.59	6.5	3.5
5-6,10	35	0.0944	25.1	—	—	0.160	25.5	43.5	0.615	6.5	3.8
8-3,140-150	50	0.0638	25.0	—	—	0.152	26.2	46.0	0.415	6.5	2.8
10-2,0-10	68	0.0779	25.0	—	—	0.151	26.4	45.9	0.506	6.5	3.3
13-6, 0-10	86	0.0913	25.2	0.0289	27.6	0.135	26.8	52.0	0.590	6.5	4.25
16-3, 140-150	93	0.0876	26.6	0.0303	27.2	0.119	26.4	58.1	0.547	6.25	4.5
18-4,140-150	130	0.0707	25.4	0.0287	27.0	0.107	25.7	65.3	0.465	6.6	4.4
21-3,140-150	157	0.0616	25.0	0.0284	25.7	0.075	25.6	95.2	0.415	6.7	5.5
23-2,140-150	170	0.0448	25.7	0.0323	25.7	0.059	25.0	136.6	0.268	6.0	4.8
24-1,135 ^a	179	0.946	31.0	0.0293	26.0	(0.051)	26.0	(150.0)	6.20	6.6	117
26-1,43 ^b	195	0.0578	25.0	0.0273	27.5	(0.047)	25.0	181	0.396	6.8	8.3
26-1,43 ^c	195	3.65	25.0	0.0450	25.0	(0.047)	25.0	181	15.9	4.4	336
28-2 ^d	215	0.0736	—	0.0282	26.0	0.0412	25.0	242	0.502	6.8	12.2
28-2 ^e	216	>100	25.0	0.0804	25.0	0.0412	25.0	246	244	2.44	>6000

Note: All measurements are in ohm-m. Measurements on sediments are on end of 10-cm liner section, where not otherwise noted. Reference fluid has $S = 35.4$ ‰, $R_w = 0.196$ at 25°C. R_s is resistivity of sediment, R_{pw} is resistivity of reference water and R_w is resistivity of reference water. C is cell constant and F is formation factor.

^aShaly anhydrite; drilling fluid in core barrel had salinity of 56.1 (resistivity 0.134) but interpolated interstitial salinity was used for measurement. Special cup shallower than 10-cm vessel used.

^bShale below first anhydrite.

^cAnhydrite.

^dShale.

^eRock salt, special-shaped vessel.

content and porosity and an increase in density. Because of the broken nature of the cores, there are rapid oscillations in the GRAPE densities, and solution effects reducing the diameter of the halite cores make the GRAPE densities somewhat unreliable. Laboratory density measurements were made on the anhydrite from this site (Wheildon et al., this volume), giving 2.83 ± 0.03 g/cm³ ($N=6$) and the density of similar halite from Site 227 was measured giving 2.14 ± 0.01 g/cm³ ($N=8$).

The core plots show that there is generally good agreement between the section weight and GRAPE densities.

The following features in the GRAPE densities on the core summary logs are noted:

Core 3 — sharp maximum at 4.5 meters is probably spurious as it does not correlate with any feature on the core photographs.

Core 4 — two minima at 6.8 and 7.8 meters are considerably lower than the section weight densities and correlate with dark patches (?) on the core photographs.

Core 9 — gentle minimum (1.6 g/cm³) followed by gentle maximum (1.9 g/cm³) followed by gentle minimum (1.6 g/cm³). The minima correlate with dark patches (? carbonaceous material) in the core photographs.

Core 11 — maximum of 1.9 g/cm³ at 8.5 meters ? correlates with light color, more lithified material in core photographs.

Core 14 — small-scale variations (minima) correlate with dark (? carbonaceous) patches in core photographs.

Core 15 — possible genuine sharp increase from 1.6 to 1.9 g/cm³ at 1.6 meters correlates with a change to more lithified material.

Core 18 — minimum at 1 meter correlates with dark (? carbonaceous material) in core photographs.

Core 19 — low values near bottom of core correlate with dark material.

Cores 20-21 — small-scale oscillations due to fragmented nature of the cores.

Core 22 — maxima correlate with white patches and minima with dark patches on core photographs.

Core 23 — maximum of 2.1 g/cm³ at 1.5 meters correlates with lighter patch in core photograph.

Cores 24, 25, 26, 27, 29 — oscillations due to fragmented evaporites (anhydrite and halite).

Compressional Wave Velocity

The sonic velocities are shown in the Site Summary and are seen to be almost constant in the Plio-Pleistocene nanno oozes (1.6 to 1.7 km/sec). With the appearance of the Miocene evaporites at 176 meters there is a sharp increase in velocity to about 4.4 km/sec and a much greater scatter is seen. The mean velocity for the evaporites is very close to the velocity of 4.49 km/sec observed at seismic refraction station 179 of Drake and Girdler (1964) and to a sonobuoy measurement of 4.5 km/sec (Ross and Schlee, in press) and likewise similar to the values for anhydrite and salt listed by Clark (1966). Further laboratory measurements of sonic velocities of anhydrite from this site are given in Wheildon et al. (this volume) in which the mean is 4.64 ± 0.71 km/sec ($N=3$).

Specific Acoustic Impedance

Throughout the Plio-Pleistocene nanno oozes, the specific acoustic impedance is seen to be fairly constant at about 3×10^6 (Nsm^{-3}). Due to the poor GRAPE determinations of densities in the evaporites, the increase in specific acoustic impedance at 176 meters is not so spectacular as it is in reality. The actual increase is by a factor of about four emphasizing the acoustic contrast between the oozes and evaporites.

Thermal Conductivity

Eighteen measurements of the thermal conductivity of the soft carbonate nanno oozes were made (Table 2, Girdler et al., this volume) giving a mean of $1.171 \pm 0.079 \text{ Wm}^{-1} \text{ K}^{-1}$. The values are shown as a function of depth (fig. 4, Girdler et al., this volume), and a much smaller scatter is seen than for Sites 227 and 228. In addition, six measurements were made on anhydrite specimens from this site (Table 1, Wheildon et al., this volume) giving a mean of $4.513 \pm 0.084 \text{ Wm}^{-1} \text{ K}^{-1}$.

HEAT FLOW MEASUREMENTS

Downhole temperatures were obtained at 19 and 78 meters subbottom. An attempt to obtain a temperature measurement at 45 meters failed, the apparatus not switching on. When the temperatures are plotted against subbottom depths, they lie on a straight line giving a thermal gradient of 92 K km^{-1} .

The temperature gradient is estimated as $92 \pm 4 \text{ K km}^{-1}$, but it is noted that this depends on only three measurements. The thermal conductivity for the depth range corresponding to the temperatures is taken as the mean of the top 10 measurements giving $1.44 \pm 0.075 \text{ W m}^{-1} \text{ K}^{-1}$, i.e., somewhat less than the mean value of $1.171 \pm 0.079 \text{ W m}^{-1} \text{ K}^{-1}$ for all the values from Site 225. The heat flow is thus $105 \pm 11 \text{ mWm}^{-2}$. These results are discussed in detail by Girdler et al. (this volume).

TABLE 7
Thermal Conductivities for Site 225

Core, Section, Depth (cm)	Subbottom Depth (cm)	Measured Conductivity ($\text{Wm}^{-1}\text{K}^{-1}$)	Corrected Conductivity ($\text{Wm}^{-1}\text{K}^{-1}$)
4-5, 100	30	1.064	1.074
5-5, 100	34	1.214	1.217
6-5, 80	43	1.211	1.222
8-2, 100	48	1.211	1.218
9-5, 80	61	0.980	0.993
10-2, 80	65	1.189	1.203
11-5, 40	78	1.123	1.143
12-1, 80	77	1.117	1.138
13-5, 75	84	1.038	1.058
15-2, 77	97	1.143	1.170
16-2, 77	106	1.231	1.262
17-3, 78	117	1.238	1.272
18-3, 68	126	1.261	1.295
19-3, 68	135	1.200	1.239
20-2, 78	142	1.087	1.123
21-2, 101	146	1.097	1.135
22-3, 65	162	1.105	1.145
23-2, 60	169	1.097	1.135

CORRELATION OF REFLECTION PROFILES AND LITHOLOGIES

A single, very strong reflector was present in the region of Site 225 (Figure 7). This reflector, named the S reflector by previous workers, is found over a wide area of the Red Sea, excluding the axial trough. Broadly the reflector is smooth and the sea bed is usually conformable with it. In detail, the reflector has an irregular surface as indicated by many small hyperbolas.

At the site the S reflector was seen at 0.20 sec. A hard layer of anhydrite, representing the top of the evaporites, was encountered at 177 meters. The mean velocity to the reflector is therefore 1.77 km/sec . The strength of the S reflector is explained by the relatively high compressional wave velocity, about 4.6 km/sec , of the anhydrite.

DISCUSSION AND CONCLUSIONS

Site 225 was drilled on the seaward edge of the marginal zone near the hot brine area. Detailed bathymetric and magnetic evidence indicates that the site is separated from the Atlantis II Deep by a north-northeast-trending transform fault (Searle et al., in preparation). Drilling went without major difficulties and we penetrated to a depth of 230 meters. Following the recommendations of the JOIDES Pollution Prevention and Safety Panel, the hole was continuously cored.

Lithology

Four distinct sedimentary units were penetrated:

Unit I: Gray foram-bearing micarb-rich detrital clayey silt nanno ooze and chalk ranging in age from late Early Pliocene to Late Pleistocene (total thickness 112 m). The sedimentation rate was 100 m/m.y. at the base of this unit and decreased 70 m/m.y. in the Late Pleistocene. During Early Pleistocene time the rate was no more than 20 m/m.y.

Unit II: Gray micarb-rich nanno detrital silty claystone of Early Pliocene age (total thickness 55 m). The sedimentation rate was about 20 m/m.y.

Unit III: Dark gray dolomitic silty claystone of Early Pliocene or Late Miocene age (total thickness 9m). The sedimentation rate was about 20 m/m.y.

Unit IV: Lithified anhydrite and halite with occasional black shale layers of presumed Late Miocene age (this unit was penetrated 54 m before drilling stopped).

The sedimentary sequence indicates Late Miocene deposition in a fairly shallow restricted basin. Reducing conditions are suggested by relatively high amounts of organic matter and pyrite in the shales of unit IV. The overlying lithologic units suggest further deepening of the basin and a connection with the Indian Ocean. Some periods of apparent isolation from the open ocean resulting in increased salinities of the surface waters are indicated by fragments of lithified carbonates in the upper 50 meters of unit I. These layers are similar to ones found in surface cores (Milliman et al., 1969) which are thought to be due to aragonite cementation during periods of higher salinity.

The sedimentation rate curve (Figure 4) indicates a marked reduction in sediment accumulation in the Early Pleistocene. An unconformity at about this time (the

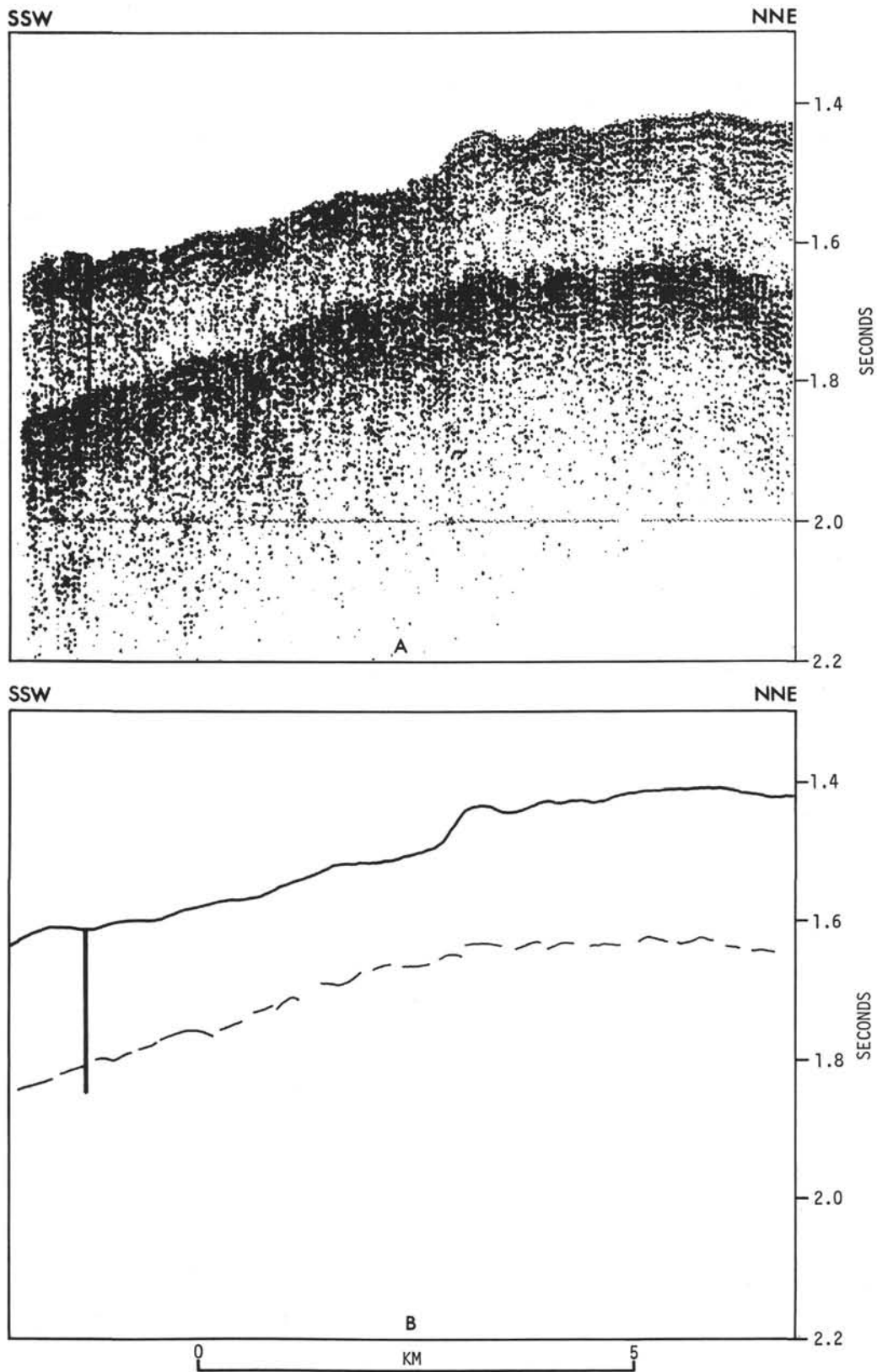


Figure 7. (a) Seismic profile obtained on the approach to Site 225. Vertical bar indicates the position of the drilled hole. (b) Line drawing interpretation of (a). The vertical bar has tenth-sec divisions.

Discoaster brouweri zone is absent) is observed at Sites 227 and 228, and seismic profiler records (Ross and Schlee, in press) also show indications of Pliocene/Pleistocene unconformities. This variation in sedimentation rates may be related to movements of the Arabian and African continents away from each other, which were thought by some to start in Pliocene-Pleistocene times (Hutchinson and Engels, 1972).

A major acoustic reflector, called reflector S, has been mapped over much of the Red Sea, except in the axial trough (Knott et al., 1966; Ross et al., 1969; Phillips and Ross, 1970; Ross and Schlee, in press). This reflector was cored at Site 225 and coincided with the top of the evaporite sequence. The acoustic velocity of the anhydrite at the top of the evaporite sequence as 4.6 km/sec, whereas the overlying sediments averaged about 1.8 km/sec. This contrast in velocity undoubtedly causes reflector S.

Paleontology

The planktonic foraminiferal fauna from Site 225 is not sufficiently diagnostic to define zones that can be correlated with other deep-sea sediments. Benthic foraminifera are not too common except in Lower Pliocene sediments, and none indicates environments deeper than neritic to upper bathyal (i.e., not deeper than present depths).

Nannofossils are fairly well represented with a complete sequence of Pleistocene and Pliocene zones present. *Discoaster quinqueramus* of Late Miocene age is found in the sediments overlying the evaporites of unit IV and gives a minimum age to this unit. Within the evaporite sequence only occasional rare diatoms, fish teeth, and benthic foraminifera were found.

Geochemistry

The geochemical analyses included the chemical composition of solids and interstitial waters. Interstitial water measurements showed increases in salinity with depth indicating that salt was present before we reached it by drilling. Some of the muds of the postevaporite sequence, analyzed by shipboard spectrographic techniques, showed iron contents as high as 5% and enrichments of vanadium and molybdenum of 1000 ppm and 500 ppm, respectively. Within the evaporite sequence, some shales contained as much as 200 ppm copper.

Recent History of the Red Sea

One of the problems of the origin and evolution of the Red Sea is concerned with just when sea-floor spreading started. The presence within 16 km of the axial trough (within 4-6 km for Site 227) of Late Miocene evaporite sediments (top is reflector S), that are overlain by a fairly thick sequence of post-Miocene sediments, bears on this question. Seismic profiles from other parts of the Red Sea can now be interpreted as showing an essentially uniform sequence of post-Miocene sediments overlying evaporites, even close to the axial trough. This observation, confirmed by all of our other Red Sea drillings, when combined with other geophysical data, suggests that the formation of the present Red Sea has taken place in at least two stages, rather than being a continuous process. The first stage

probably occurred in pre-Miocene times, the second movement has occurred over about the last 3 m.y. and is responsible for the axial trough. Several mechanisms have been suggested to explain the initial formation of the Red Sea basin but two seem more probable:

- 1) An uplift forming a graben (Cloos, 1939).
- 2) A depression resulting from the movement of Saudi Arabia away from Africa (Swartz and Arden, 1960; Drake and Girdler, 1964; Falcon et al., 1970; Allan and Morelli, 1970).

Seismic reflection data do not clearly favor either of these two mechanisms. The frequent absence of pre-Miocene sediments above the igneous basement suggests that the area may have been a topographic high during the Paleogene. A main reason for suggesting only recent sea-floor spreading is that the sediment above reflector S (the pre-Pliocene evaporites) generally has a fairly uniform thickness with little evidence of thinning toward the axial trough (Ross and Schlee, in press) and then abruptly thins and essentially disappears in the axial trough. If spreading had been continuous, we would have expected a decreased thickness of sediment toward the axial zone, i.e., the area of spreading.

It is of interest that reflector S in the Red Sea has an age similar to that of reflector M mapped over much of the Mediterranean (Ryan et al., 1973), and both are due to evaporites. Thus, both areas were evaporite basins during the Miocene, and indeed may even have been connected. Evidence presented elsewhere (Manheim, Chapter 38; Stoffers and Kühn, this volume) suggests that the Miocene Red Sea was a fairly shallow sea; Friedman (1972) has suggested that it was a marginal-flat or sabkha. At or near the end of the Miocene, evaporite conditions disappeared and normal marine conditions replaced them. Seismic profiles indicate some tectonic activity, especially to the north near the Sinai peninsula and in the south where movements resulted in the formation of the Straits of Bab el Mandeb (Abdel-Gawad, 1970). Sediments and their fauna indicate increased water depth from Early Pliocene until recent times, with reducing conditions prevailing occasionally.

There are also indications that sea-level changes occurred in post-Miocene times. In particular, lithified carbonates found in the upper Pleistocene section indicate periods of increased salinity in the Red Sea due to glacial lowering of sea level or tectonic movements which restricted inflow of Indian Ocean water over the shallow (less than about 150 m) sill at the Straits of Bab el Mandeb.

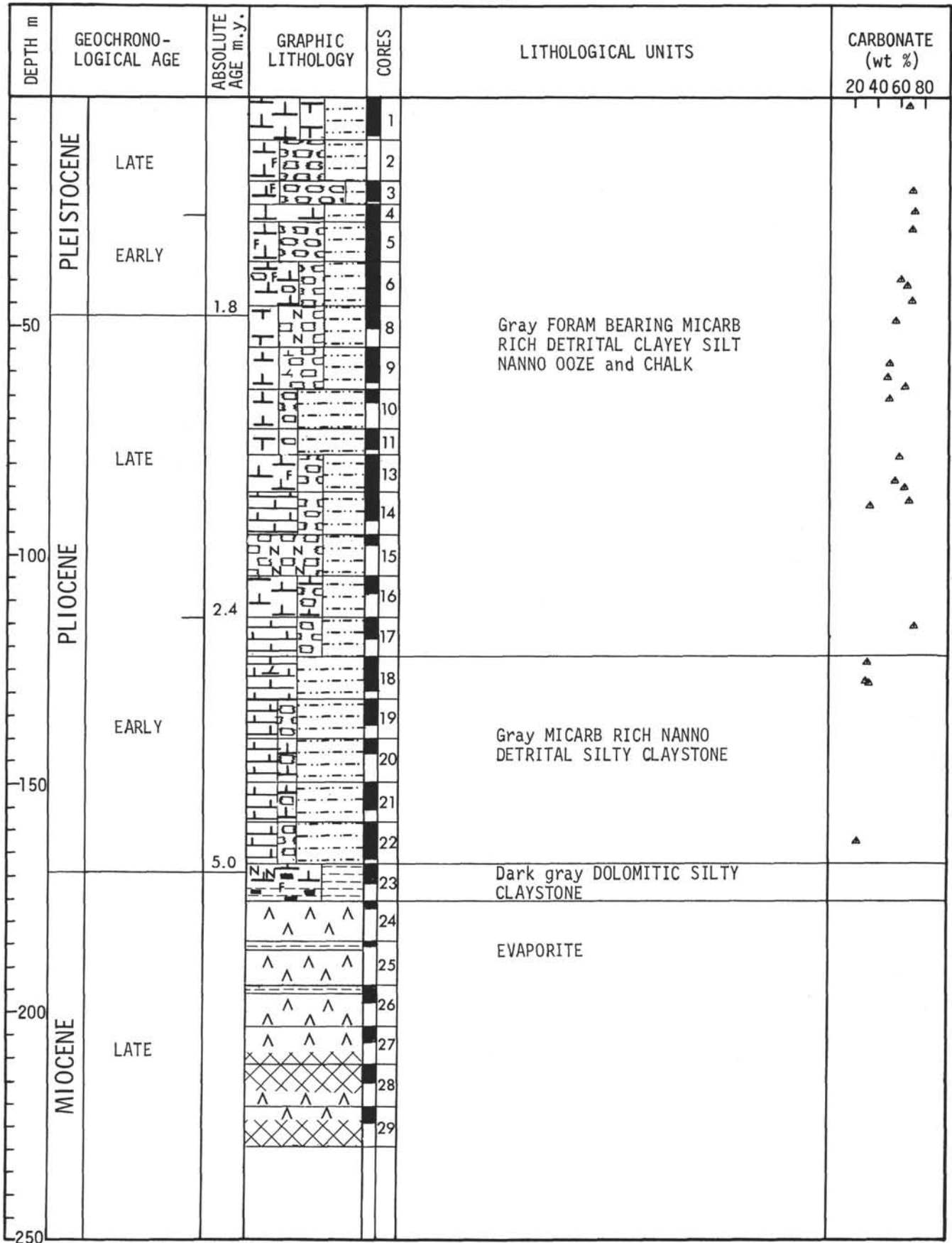
There was no evidence of chemical alteration or other effects of the nearby hot brines on the sediments and rocks cored at Site 225. Nor were any ancient brine deposits found. However, the vanadium and molybdenum enrichments in some of the dark muds and shales reached values generally only found in ores such as the Kupferschiefer.

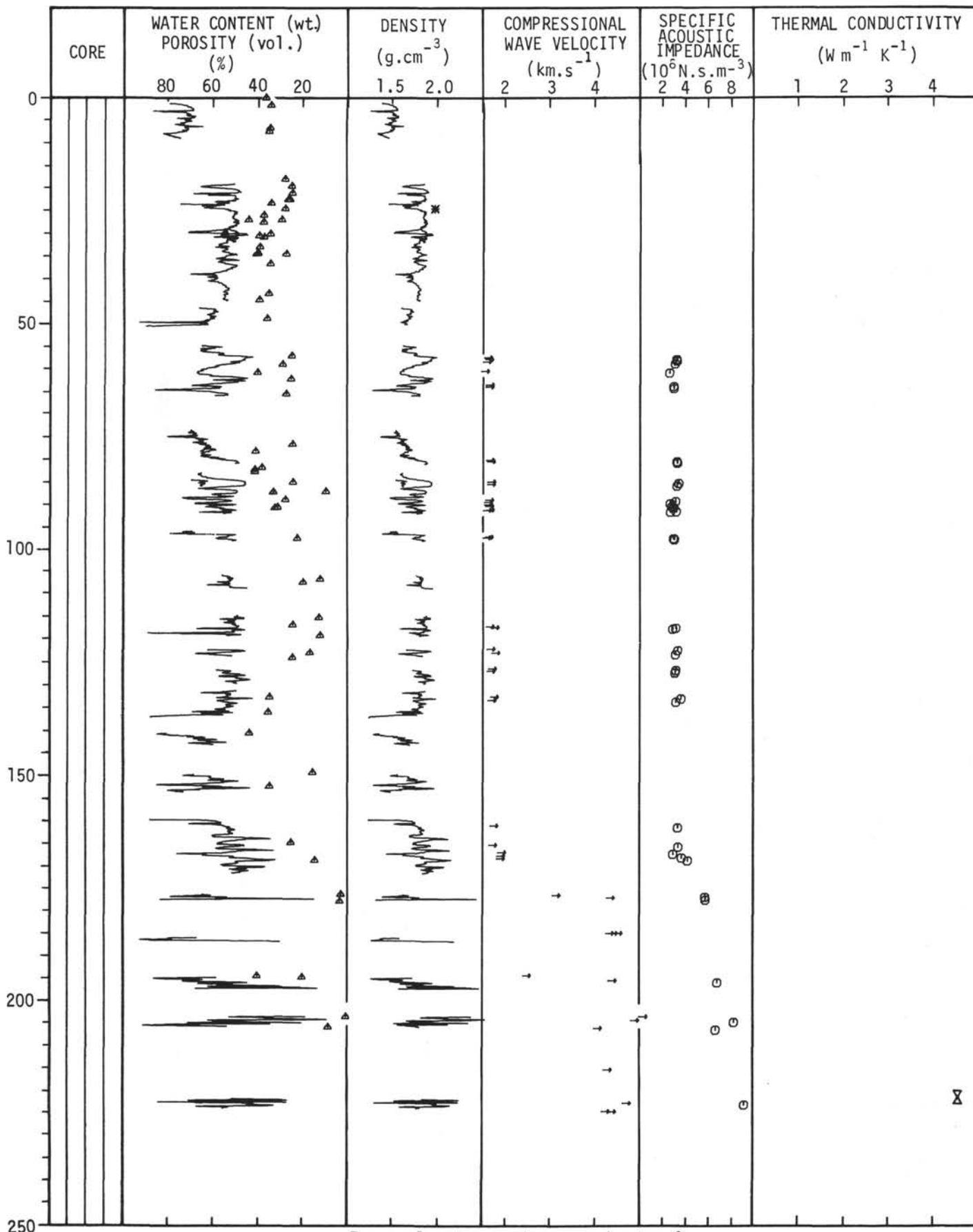
REFERENCES

- Abdel-Gawad, M., 1970. The Gulf of Suez: A brief review of stratigraphy and structure: Phil. Trans. Roy. Soc. London, Series A, v. 267, p. 41-47.
- Allan, T. D., 1966. A bathymetric chart of the Red Sea; Int. Hyd. Rev., v. 43, p. 33-36.

- Allan, T. D. and Morelli, C., 1970. The Red Sea. *In* The Sea: New York (Wiley-Interscience), p. 493-542.
- Amann, H., 1972. Marine raw material exploration with the 'Valdivia': *Meerestechnik*, v. 3, p. 102-106.
- Berggren, W. A. and Boersma, A., 1969. Late Pleistocene and Holocene planktonic foraminifera from the Red Sea. *In* Degens, E. T. and Ross, D. A. (Eds.), *Hot brines and recent heavy metal deposits in the Red Sea*: New York (Springer-Verlag), p. 282-298.
- Bischoff, J. L. and Manheim, F. T., 1969. Economic potential of the Red Sea heavy metal deposits. *In* Degens, E. T. and Ross, D. A. (Eds.), *Hot brines and recent heavy metal deposits in the Red Sea*: New York (Springer-Verlag), p. 535-541.
- Boudreaux, J. E. and Hay, W. H., 1969. Calcareous nannoplankton and biostratigraphy of the Late Pliocene-Pleistocene-Recent sediments in the Submarex cores: *Rev. Espanola Micropaleontologia*, v. 1, p. 249-292.
- Bukry, D., 1971. Cenozoic calcareous nannofossils from the Pacific Ocean: *San Diego Soc. Nat. Hist. Trans.*, v. 16, p. 303-327.
- Clark, S. P., Jr. (Ed), 1966. *Handbook of physical constants*: New York (Geological Society of America, Inc.).
- Cloos, H., 1939. *Hebung-Spaltung-Vulcanismus*: *Geol. Rdsch.*, v. 30, p. 405.
- Degens, E. T. and Ross, D. A., (Eds.), 1969. *Hot brines and recent Heavy metal deposits in the Red Sea*: New York (Springer-Verlag).
- Drake, C. L. and Girdler, R. W., 1964. A geophysical study of the Red Sea: *Geophy. J. Roy. Astr. Soc.*, v. 8, p. 473-495.
- Erickson, A. J. and Simmons, G., 1969. Thermal measurements in the Red Sea hot brine pools. *In* Degens, E. T. and Ross, D. A. (Eds.), *Hot brines and recent heavy metal deposits in the Red Sea*: New York (Springer-Verlag), p. 114-121.
- Fairhead, J. D. and Girdler, R. W., 1970. The seismicity of the Red Sea, Gulf of Aden, and Afar Triangle: *Phil. Trans. Roy. Soc. London, Series A*, v. 267, p. 49-71.
- Falcon, N. L., Gass, I. G., Girdler, R. W., and Laughton, A. S., 1970. A discussion on the structure and evolution of the Red Sea and the nature of the Red Sea, Gulf of Aden, and Ethiopia Rift Junction: *Phil. Trans. Roy. Soc. London, Series A*, v. 267, p. 417.
- Friedman, G. M., 1972. Significance of Red Sea in problem of evaporites and basinal limestones: *Am. Assoc. Petrol. Geol. Bull.*, v. 56, p. 1072-1086.
- Girdler, R. W., 1970. A review of the Red Sea heat flow: *Phil. Trans. Roy. Soc. London, Series A*, v. 267, p. 191.
- Hutchinson, R. W. and Engels, G. G., 1972. Tectonic evolution in the southern Red Sea and its possible significance to older rifted continental margins: *Geol. Soc. Am. Bull.*, v. 83, p. 2989-3002.
- Knott, S. T., Bunce, T., and Chase, R. L., 1966. Red Sea seismic reflection: The world rift system: *Geol. Survey Canada Paper* 66-14, p. 5.
- Laughton, A. S., 1970. A new bathymetric chart of the Red Sea: *Phil. Trans. Roy. Soc. London, Series A*, v. 267, p. 21-22.
- Lowell, J. D. and Genik, G. J., 1972. Sea-floor spreading and structural evolution of southern Red Sea: *Am. Assoc. Petrol. Geol. Bull.*, v. 56, p. 247-259.
- Milliman, J. D., Ross, D. A., and Ku, T. L. 1969. Precipitation and lithification of deep-sea carbonates in the Red Sea: *J. Sediment. Petrol.*, v. 39, p. 724-736.
- Phillips, J. D. and Ross, D. A., 1970. Continuous seismic reflexion profiles in the Red Sea: *Phil. Trans. Roy. Soc. London, Series A*, v. 267, p. 143-152.
- Ross, D. A., Hays, E. E., and Allstrom, F. C., 1969. Bathymetry and continuous seismic profiles of the hot brine region of the Red Sea. *In* Degens, E. T. and Ross, D. A. (Eds.), *Hot brines and recent heavy metal deposits in the Red Sea*: New York (Springer-Verlag), p. 82-97.
- Ross, D. A. and Schlee, J., in press. Recent geological history of the southern Red Sea: *Geol. Soc. Am. Bull.*
- Ryan, W. B. F., Hsü, K. J., Nesteroff, W. D., Pautot, G., Wezel, F. C., Lort, J. M., Cita, M. B., Maync, W., Stradner, H., and Dumitrica, P., 1970. Deep sea drilling project: Leg 13: *Geotimes*, v. 15, p. 12-15.
- Searle, R. C., Ross, D. A., Phillips, J. D., in preparation. Magnetic anomalies and recent sea floor spreading in the central Red Sea.
- Swartz, D. H. and Arden, D. D., Jr., 1960. Geologic history of the Red Sea area: *Am. Assoc. Petrol. Geol. Bull.*, v. 44, p. 1621-1637.
- Vine, F. J., 1966. Spreading of the ocean floor - new evidence: *Science*, v. 154, p. 1405-1415.

SITE 225





For explanatory notes see chapter 2.

Site 225 Hole Core 1 Cored Interval: 0-9 m

AGE	ZONE	FOSSIL CHARACTER				SECTION METERS	LITHOLOGY	DEFORMATION	LITHO. SAMPLE	LITHOLOGIC DESCRIPTION
		FORAMS	NANNOS	RADS	OTHERS					
LATE PLEISTOCENE	Gephyrocapsa oceanica	abundant, well preserved	common and well preserved	absent	0.5	[Lithology symbols]	[Deformation symbols]	80	1	Yellowish brown DETRITAL CLAYEY SILT - FORAM RICH MICARB NANNO OOZE.
					1					Soupy, intensely deformed by drilling semilithified grains ranging in size from sand to granule occur irregularly throughout the section.
					1.0					
	Gephyrocapsa caribbeantica	abundant, well preserved	common and well preserved	absent	2	[Lithology symbols]	[Deformation symbols]	68	2	Dominant lithology SS: Section 3-75 cm. DETRITAL CLAYEY SILT - FORAM RICH MICARB NANNO OOZE Composition: Nannos 35% Micarb 25% Forams 20% Detrital 20% Texture: Silt 70% Clay 30%
					3					Color legend: 1 = gray orange 10YR 7/4 2 = yellowish gray 5Y 7/2 3 = light yellowish brown 10YR 6/4
	Gephyrocapsa caribbeantica	abundant, well preserved	common and well preserved	absent	4	[Lithology symbols]	[Deformation symbols]	75	3	Shore-based laboratory results Organic Carbon Carbonate Section 2-40 cm = .1% 67% Grain Size: Section 2-41 cm Sand 1% Silt 58% Clay 41% X-ray mineralogy: Section 2-50 cm Calcite 20% Dolomite 2% Mg-Calcite 60% Quartz 7% K-feldspar 2% Plagioclase 5% Mica 4% Chlorite 1%
5										
					6	[Lithology symbols]	60	3		
					Core Catcher	[Lithology symbols]		CC	2	

Explanatory notes in chapter 2

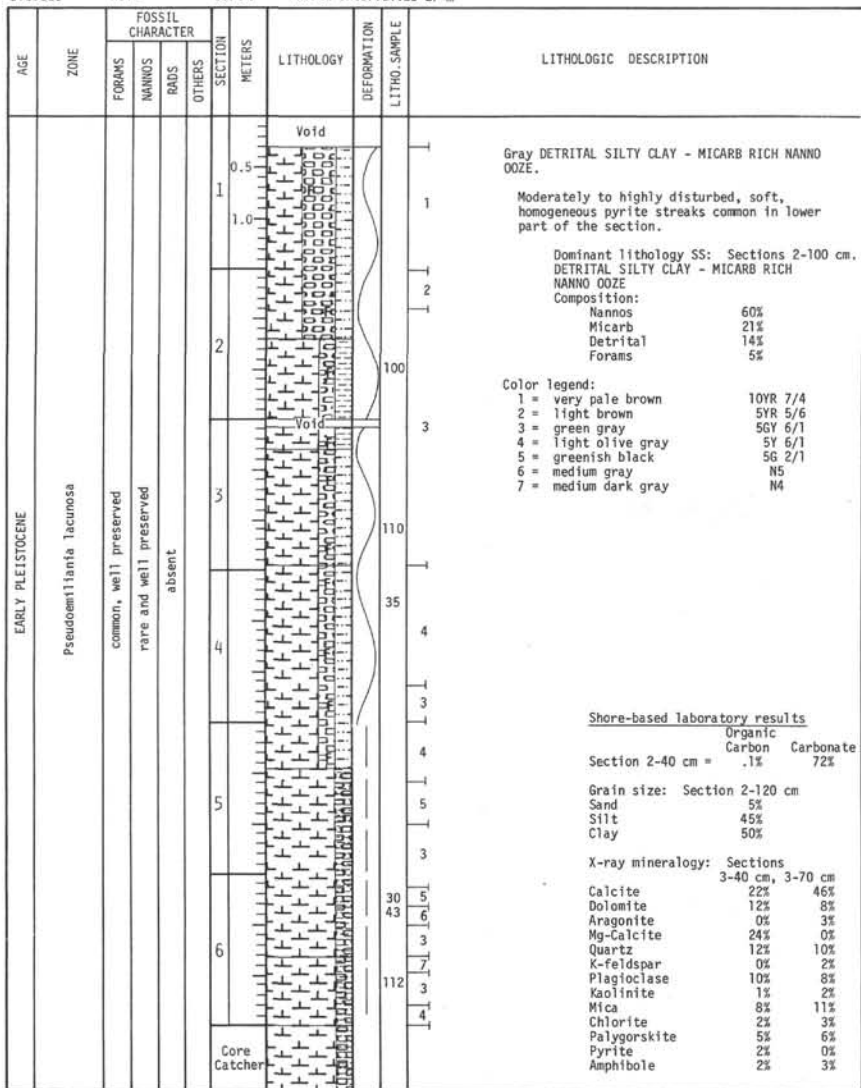
Site 225 Hole Core 2 Cored Interval: 9-18 m

AGE	ZONE	FOSSIL CHARACTER				SECTION METERS	LITHOLOGY	DEFORMATION	LITHO. SAMPLE	LITHOLOGIC DESCRIPTION
		FORAMS	NANNOS	RADS	OTHERS					
LATE PLEISTOCENE	Gephyrocapsa caribbeantica	few, well preserved	common and well preserved	absent	Core Catcher	[Lithology symbols]	[Deformation symbols]		1	Yellowish gray DETRITAL CLAYEY SILT - NANNO RICH MICARB OOZE. Dominant lithology SS: Section CC. DETRITAL CLAYEY SILT - NANNO RICH MICARB OOZE Composition: Micarb 55% Nannos 25% Detrital 20% Texture: Silt 65% Clay 35% Color legend: 1 = yellowish gray 5Y 7/2

Site 225 Hole Core 3 Cored Interval: 18-23 m

AGE	ZONE	FOSSIL CHARACTER				SECTION METERS	LITHOLOGY	DEFORMATION	LITHO. SAMPLE	LITHOLOGIC DESCRIPTION
		FORAMS	NANNOS	RADS	OTHERS					
LATE PLEISTOCENE	Coccolithus doronicoides	common, well preserved	rare, and moderately well preserved	absent	0.5	[Lithology symbols]	[Deformation symbols]	140	1	Greenish gray DETRITAL CLAYEY SILT - NANNO RICH MICARB OOZE. Soft, highly deformed, homogeneous. Few pyrite streaks. Dominant lithology SS: Section 3-100 cm. DETRITAL CLAYEY SILT - NANNO RICH MICARB OOZE Composition: Micarb 60% Detrital 20% Nannos 10% Forams 10% Texture: Silt 70% Clay 30%
					1					Void
					1.0					
					2					
					3					Void
					4					Void
					Core Catcher	[Lithology symbols]		CC	2	Shore-based laboratory results Organic Carbon Carbonate Section 2-90 cm = .1% 70% Grain size: Section 2-115 cm Sand 5% Silt 45% Clay 50% X-ray mineralogy: Section 3-100 cm Calcite 26% Dolomite 6% Aragonite 1% Mg-Calcite 36% Quartz 8% K-feldspar 3% Plagioclase 10% Kaolinite 2% Mica 7% Chlorite 2% Amphibole 2%

Explanatory notes in chapter 2



Site 225 Hole Core11 Cored Interval:72-77 m

AGE	ZONE	FOSSIL CHARACTER			SECTION METERS	LITHOLOGY	DEFORMATION	LITHO. SAMPLE	LITHOLOGIC DESCRIPTION
		FORAMS	NANNOS	RADS					
LATE PLIOCENE	Discoaster surculus	abundant, well preserved	abundant and well preserved	absent	0.5	Void		Greenish gray DETRITAL CLAY FORAM RICH MICARB OOZE with minor interbeds of olive gray to olive black DETRITAL CLAY - NANNO RICH MICARB OOZE.	
					1.0		Moderately to very intensely deformed. Soupy to soft.		
					2		Dominant lithology SS: Section 4-61 cm. DETRITAL CLAY FORAM RICH MICARB OOZE Composition: Micarb 68% Forams 18% Detrital 12% Dolomite 2%		
					3	1 with mottles of 2	SS: Section 5-72 cm. DETRITAL CLAY - NANNO RICH MICARB OOZE Composition: Micarb 40% Detrital 30% Nannos 20% Forams 10%		
					4	1	Color legend: 1 = light greenish gray 5G 8/1 2 = olive black 5Y 2/1 3 = dark olive gray 5Y 3/2		
					5	3			
					61	1			
					72	3			
							1	3 with few mottles of 1	
							1	1 with few mottles of 3	
							CC	Core Catcher	

Explanatory notes in chapter 2

Site 225 Hole Core12 Cored Interval:77-77 m

AGE	ZONE	FOSSIL CHARACTER			SECTION METERS	LITHOLOGY	DEFORMATION	LITHO. SAMPLE	LITHOLOGIC DESCRIPTION
		FORAMS	NANNOS	RADS					
LATE PLIOCENE	Discoaster surculus	abundant and well preserved		absent	0.5	Void		Yellowish green DOLomite MICARB RICH NANNO OOZE.	
					1.0		115	Soft, intensely disturbed.	
							CC	Dominant lithology SS: Section 1-115 cm. Composition: Nannos 50% Micarb 25% Dolomite 15% Detrital 6% Forams 4%	
								Color legend: 1 = yellowish green 5G 5/2	
								<u>Shore-based laboratory results</u> Organic Carbon Carbonate Section 1-105 cm = 1.3% 59%	
								Grain size: Section 1-110 cm Sand 30% Silt 35% Clay 35%	

Explanatory notes in chapter 2

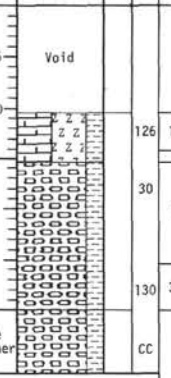
AGE	ZONE	FOSSIL CHARACTER				SECTION METERS	LITHOLOGY	DEFORMATION	LITHO. SAMPLE	LITHOLOGIC DESCRIPTION
		FORAMS	NANNOS	RADS	OTHERS					
LATE PLIOGENE	Discoaster surculus	common, well preserved	abundant and well preserved	absent						
					0.5				Yellowish green DETRITAL SILTY CLAY RICH - MICARB NANNO OOZE.	
					1			2 & 3	Soupy to soft, intensely disturbed and mottled by drilling. Upper part of the section contains sand-sized semilithified carbonate grains. Pyrite streaks are common in the lower part of section.	
					2			70	Dominant lithology SS: Sections 2-70 cm, 2-120 cm. DETRITAL SILTY CLAY RICH - MICARB NANNO OOZE	
					3			120	Composition: Nannos 40% Carbonates 30% Detrital 15% Forams 10% Dolomite 5%	
					4			1	Color legend: 1 = yellowish green 5GY 5/2 2 = grayish olive green 5GY 3/2 3 = pale yellow green 10GY 7/2 4 = pale green 10G 6/2	
					5			dominantly	<u>Shore-based laboratory results</u> Organic Carbon Carbonate Section 5-35 cm = 1.4% 55% Section 6-33 cm = .1% 63%	
					6			4	Grain size: Sections 5-25 cm 6-28 cm Sand 11% 14% Silt 43% 47% Clay 46% 39%	
					Core Catcher			129	X-ray mineralogy: Section 6-30 cm Calcite 54% Dolomite 17% Quartz 5% K-feldspar 1% Plagioclase 7% Mica 7% Chlorite 2% Palygorskite 5% Pyrite 2%	

Explanatory notes in chapter 2

AGE	ZONE	FOSSIL CHARACTER				SECTION METERS	LITHOLOGY	DEFORMATION	LITHO. SAMPLE	LITHOLOGIC DESCRIPTION
		FORAMS	NANNOS	RADS	OTHERS					
LATE PLIOGENE	Discoaster surculus	common, well preserved	common and moderately well preserved	absent						
					0.5	Void			Greenish gray DETRITAL SILTY CLAY RICH NANNO MICARB CHALK with minor interbeds of olive gray MICARB DETRITAL SILTY CLAY RICH - NANNO CHALK.	
					1			128	Semilithified, slightly bioturbated. Pyrite blebs and pyrite aggregates common throughout the section.	
					2			70	Dominant lithology SS: Section 2-70 cm. DETRITAL SILTY CLAY RICH NANNO MICARB CHALK	
					3			120	Composition: Micarb 50% Nannos 30% Detrital 12% Dolomite 5% Forams 3%	
					4			1	SS: Section 2-120 cm MICARB DETRITAL SILTY CLAY RICH - NANNO CHALK	
					5			1	Composition: Nannos 73% Detrital 15% Micarb 12%	
					6			1	Color legend: 1 = light greenish gray 5G 8/1 2 = gray olive green 5GY 3/2 3 = light olive gray 5Y 6/1 4 = greenish gray 5G 6/1	
					7			2	<u>Shore-based laboratory results</u> Organic Carbon Carbonate Section 2- 35 cm = .2% 67% Section 2-133 cm = 6.2% 34%	
					8			4	Grain size: Section 2-45 cm Sand 2% Silt 49% Clay 49%	
					Core Catcher			CC	X-ray mineralogy: Sections 2-40 cm, 3-120 cm, 4-60 cm Calcite 69% 43% 65% Dolomite 10% 11% 9% Quartz 4% 9% 5% K-feldspar 1% 1% 3% Plagioclase 2% 12% 4% Kaolinite 1% 0% 0% Mica 6% 9% 7% Chlorite 1% 2% 1% Montmorillonite 1% 5% 0% Palygorskite 1% 9% 7%	

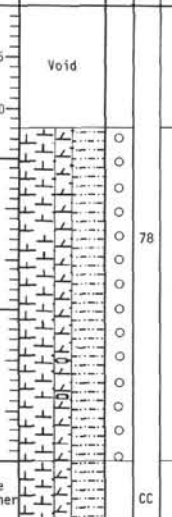
Explanatory notes in chapter 2

Site 225 Hole Core15 Cored Interval:95-104 m

AGE	ZONE	FOSSIL CHARACTER			SECTION METERS	LITHOLOGY	DEFORMATION	LITHO. SAMPLE	LITHOLOGIC DESCRIPTION
		FORAMS	NANNOS	OTHERS					
LATE PLIOCENE	Sphenolithus abies	planctonics absent	abundant and well preserved	absent	0.5 1 1.0 2 Core Catcher	Void 	1 2 1 3 CC	Greenish gray DETRITAL CLAY RICH - MICARB CHALK with minor intercalations of greenish gray DETRITAL CLAY RICH - ZEOLITE NANNO CHALK. Semilithified. Upper part slightly bioturbated. Dominant lithology SS: Section 2-30 cm. DETRITAL CLAY RICH - MICARB CHALK Composition: Micarb 80% Detrital 20% Minor lithology SS: Section 1-126 cm DETRITAL CLAY RICH - ZEOLITE NANNO CHALK Composition: Nannos 35% Zeolite 30% Detrital 25% Forams 5% Micarb 5% Color legend: 1 = greenish gray 5GY 6/1 2 = light gray 2.5Y 7/1 3 = light greenish gray 5GY 8/1 <u>Shore-Based laboratory results</u> Grain size: Section 2-122 cm Sand Trace Silt 58% Clay 42% X-ray mineralogy: Section 1-130 cm Calcite 39% Dolomite 3% Quartz 5% Plagioclase 6% Mica 2% Montmorillonite 13% Clinoptilolite 1% Phillipsite 29% Pyrite 2%	

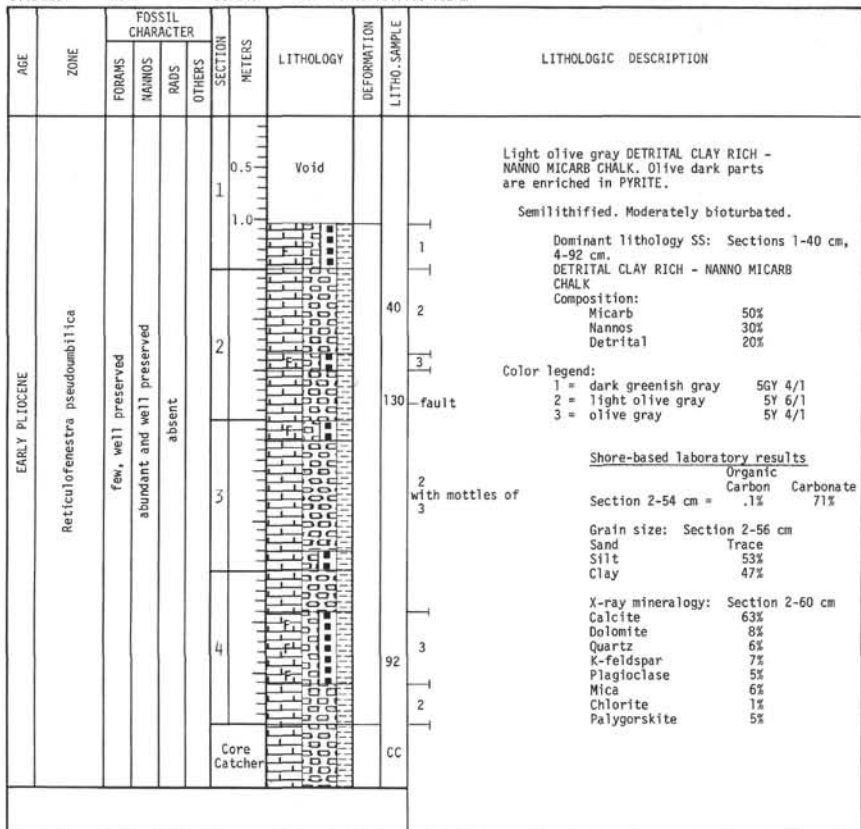
Explanatory notes in chapter 2

Site 225 Hole Core16 Cored Interval:104-113 m

AGE	ZONE	FOSSIL CHARACTER			SECTION METERS	LITHOLOGY	DEFORMATION	LITHO. SAMPLE	LITHOLOGIC DESCRIPTION
		FORAMS	NANNOS	OTHERS					
LATE PLIOCENE	Sphenolithus abies	common, well preserved	abundant and well preserved	absent	0.5 1 1.0 2 3 Core Catcher	Void 	1 78 1 CC	Olive gray DOLOMITE RICH - DETRITAL CLAY - NANNO OOZE Soft, brecciated by drilling. Dominant lithology SS: 2-78 cm. DOLOMITE RICH - DETRITAL SILTY CLAY - NANNO OOZE Composition: Nannos 40% Detrital 40% Dolomite 13% Micarb 7% Color legend: 1 = light olive gray 5Y 6/1	

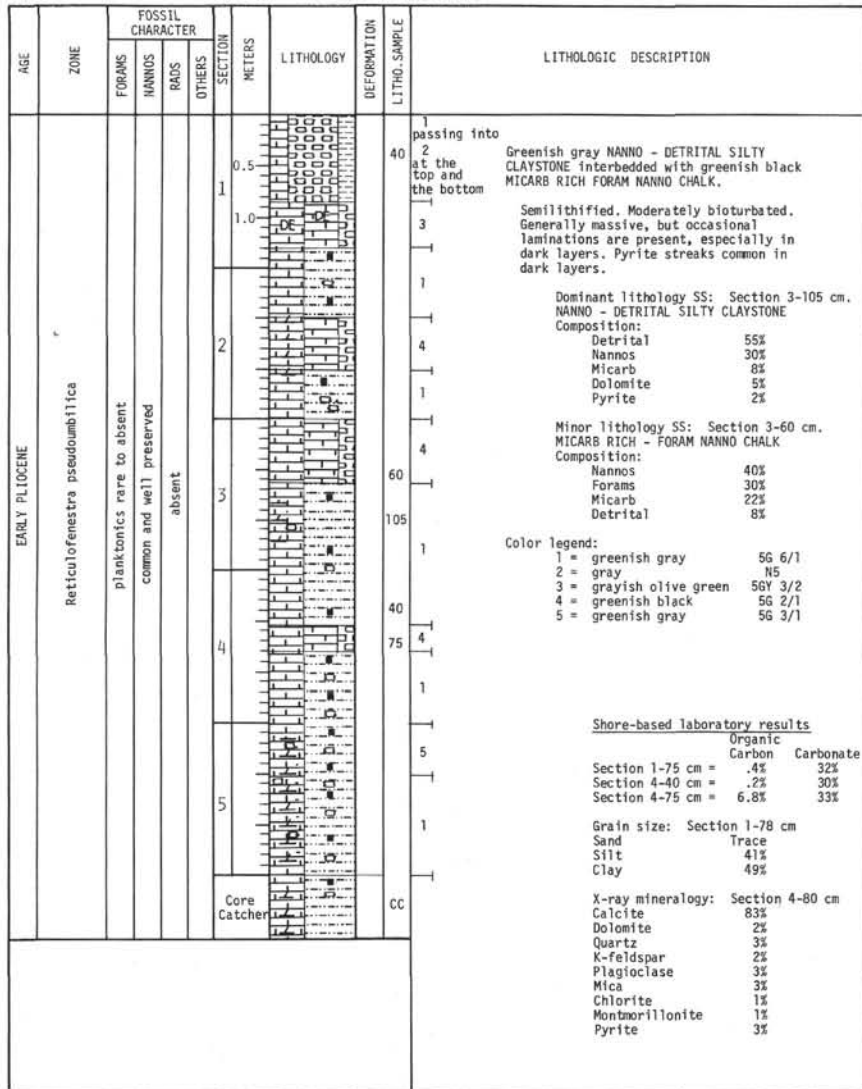
Explanatory notes in chapter 2

Site 225 Hole Core17 Cored Interval:113-122 m



Explanatory notes in chapter 2

Site 225 Hole Core18 Cored Interval:122-131 m



Explanatory notes in chapter 2

Site 225 Hole Core 25 Cored Interval: 185-194 m

AGE	ZONE	FOSSIL CHARACTER				SECTION METERS	LITHOLOGY	DEFORMATION	LITHO. SAMPLE	LITHOLOGIC DESCRIPTION																					
		FORAMS	NANNOS	RADS	OTHERS																										
MIOCENE?		absent	absent	absent				65 93 CC	<p>White ANHYDRITE interbedded with black PYRITE RICH DOLOMITIC SILTY CLAYSTONE and gray CLAYEY GYPSIFEROUS DOLOMITE.</p> <p>Semilithified.</p> <p>Dominant lithology SS: Sections 1-65 cm, 1-93 cm. PYRITE RICH DOLOMITE SILTY CLAYSTONE</p> <p>Composition:</p> <table border="0"> <tr><td>Detrital</td><td>60%</td></tr> <tr><td>Dolomite</td><td>30%</td></tr> <tr><td>Pyrite</td><td>10%</td></tr> </table> <p>CLAYEY GYPSIFEROUS DOLOMITE</p> <p>Composition:</p> <table border="0"> <tr><td>Dolomite</td><td>60%</td></tr> <tr><td>Detrital</td><td>20%</td></tr> <tr><td>Gypsum</td><td>15%</td></tr> <tr><td>Pyrite</td><td>5%</td></tr> </table> <p>Color legend:</p> <table border="0"> <tr><td>1 = white</td><td>N9</td></tr> <tr><td>2 = olive black</td><td>5Y 2/1</td></tr> <tr><td>3 = yellowish gray</td><td>5GY 5/2</td></tr> <tr><td>4 = dark gray</td><td>N3</td></tr> </table>	Detrital	60%	Dolomite	30%	Pyrite	10%	Dolomite	60%	Detrital	20%	Gypsum	15%	Pyrite	5%	1 = white	N9	2 = olive black	5Y 2/1	3 = yellowish gray	5GY 5/2	4 = dark gray	N3
Detrital	60%																														
Dolomite	30%																														
Pyrite	10%																														
Dolomite	60%																														
Detrital	20%																														
Gypsum	15%																														
Pyrite	5%																														
1 = white	N9																														
2 = olive black	5Y 2/1																														
3 = yellowish gray	5GY 5/2																														
4 = dark gray	N3																														

Site 225 Hole Core 26 Cored Interval: 194-203 m

AGE	ZONE	FOSSIL CHARACTER				SECTION METERS	LITHOLOGY	DEFORMATION	LITHO. SAMPLE	LITHOLOGIC DESCRIPTION											
		FORAMS	NANNOS	RADS	OTHERS																
MIOCENE?		absent	absent	absent				5 50 3 CC	<p>White ANHYDRITE and black PYRITE DOLOMITIC SILTY CLAYSTONE.</p> <p>Semilithified.</p> <p>Dominant lithology SS: Section 1-50 cm. PYRITE DOLOMITIC SILTY CLAYSTONE</p> <p>Composition:</p> <table border="0"> <tr><td>Detrital</td><td>70%</td></tr> <tr><td>Pyrite</td><td>15%</td></tr> <tr><td>Dolomite</td><td>15%</td></tr> </table> <p>Color legend:</p> <table border="0"> <tr><td>1 = black</td><td>N1</td></tr> <tr><td>2 = dark greenish gray</td><td>5GY 4/1</td></tr> <tr><td>3 = white</td><td>N9</td></tr> </table>	Detrital	70%	Pyrite	15%	Dolomite	15%	1 = black	N1	2 = dark greenish gray	5GY 4/1	3 = white	N9
Detrital	70%																				
Pyrite	15%																				
Dolomite	15%																				
1 = black	N1																				
2 = dark greenish gray	5GY 4/1																				
3 = white	N9																				

Explanatory notes in chapter 2

Site 225 Hole Core 27 Cored Interval: 203-212 m

AGE	ZONE	FOSSIL CHARACTER				SECTION METERS	LITHOLOGY	DEFORMATION	LITHO. SAMPLE	LITHOLOGIC DESCRIPTION			
		FORAMS	NANNOS	RADS	OTHERS								
?		absent	absent	absent				1 2 1 CC	<p>White ANHYDRITE and HALITE.</p> <p>Anhydrites are laminated to nodular.</p> <p>Color legend:</p> <table border="0"> <tr><td>1 = white</td><td>N9</td></tr> <tr><td>2 = dusky yellow green</td><td>5GY 5/2</td></tr> </table>	1 = white	N9	2 = dusky yellow green	5GY 5/2
1 = white	N9												
2 = dusky yellow green	5GY 5/2												

Site 225 Hole Core 28 Cored Interval: 212-221 m

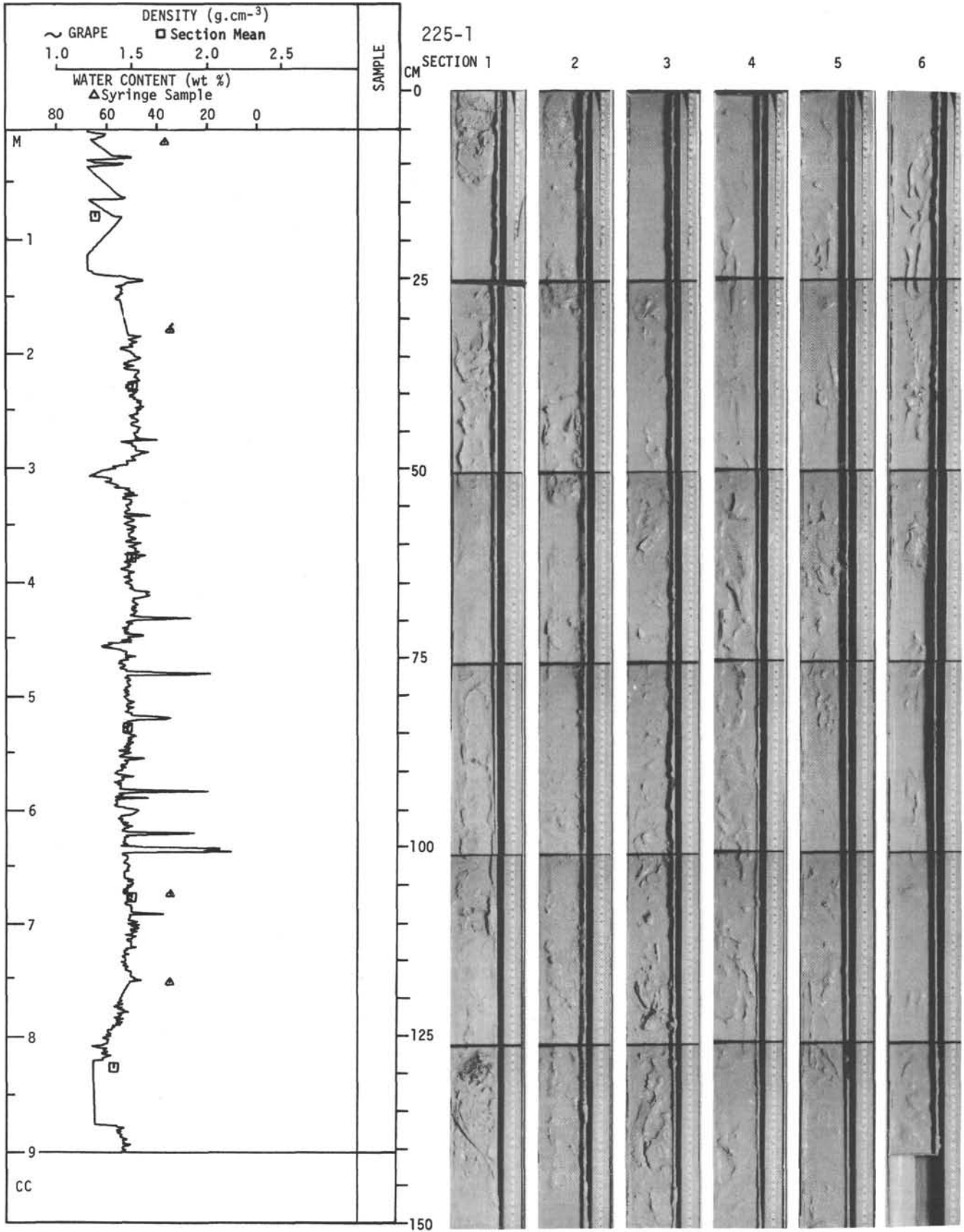
AGE	ZONE	FOSSIL CHARACTER				SECTION METERS	LITHOLOGY	DEFORMATION	LITHO. SAMPLE	LITHOLOGIC DESCRIPTION	
		FORAMS	NANNOS	RADS	OTHERS						
?		absent	absent	absent				1 2 3 CC	<p>Laminated HALITE - ANHYDRITE and nodular ANHYDRITE.</p> <p>Laminae show dip of = 15-20°.</p> <p>Color legend:</p> <table border="0"> <tr><td>1 = white</td><td>N9</td></tr> </table>	1 = white	N9
1 = white	N9										

Explanatory notes in chapter 2

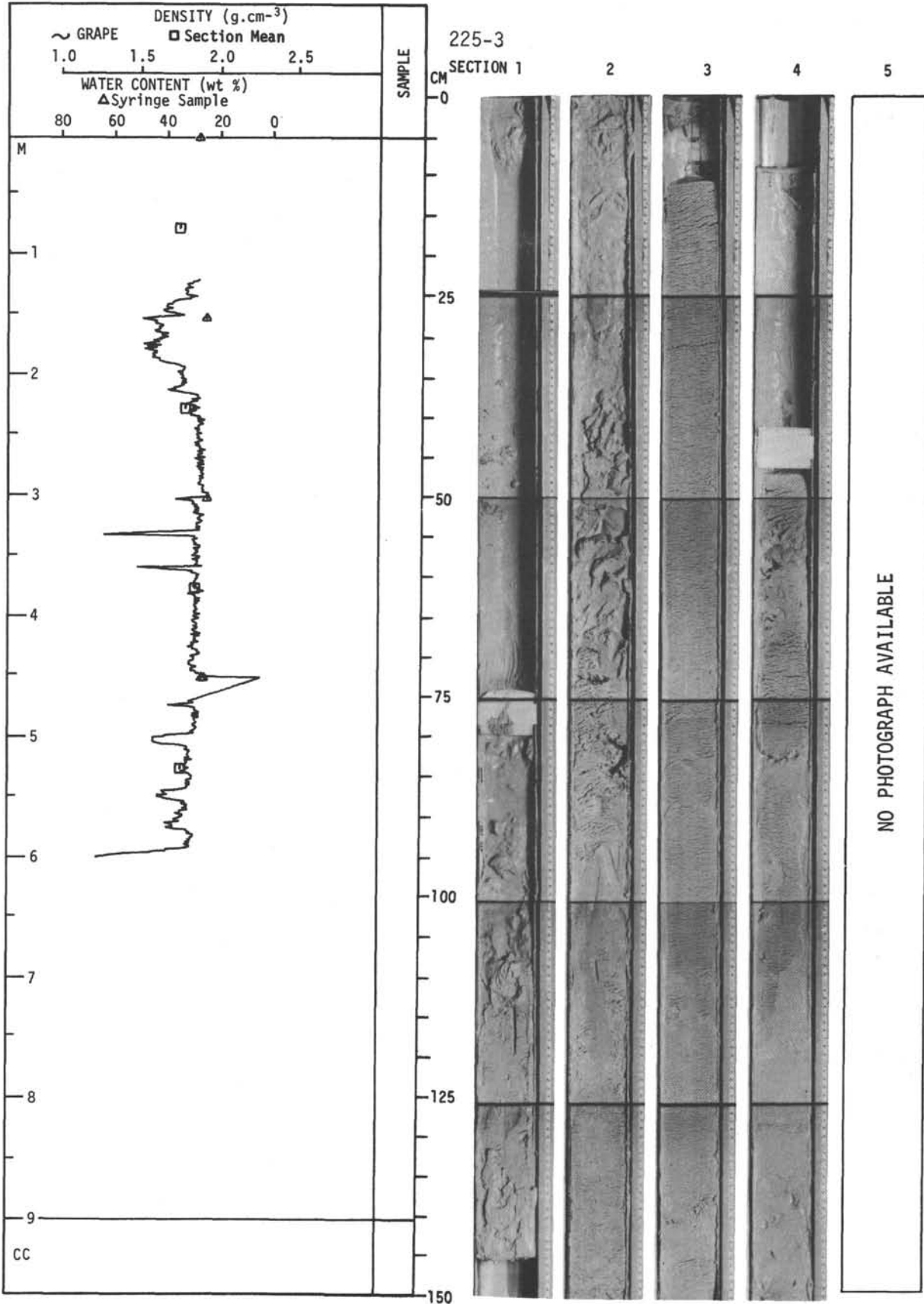
Site 225 Hole Core 29 Cored Interval: 221-230 m

AGE	ZONE	FOSSIL CHARACTER				SECTION METERS	LITHOLOGY	DEFORMATION	LITHO. SAMPLE	LITHOLOGIC DESCRIPTION
		FORBAMS	NANNOS	RADIS	OTHERS					
		absent	absent	absent		<p>Void</p> <p>0.5</p> <p>1</p> <p>1.0</p> <p>2</p> <p>3</p> <p>Core Catcher</p>		1 65 2 CC	<p>Coarse nodular ANHYDRITE and laminated HALITE - ANHYDRITE.</p> <p>Anhydrite laminae in Halite show 10-15° dip.</p> <p>Color legend: 1 = black N1 2 = white N9</p>	

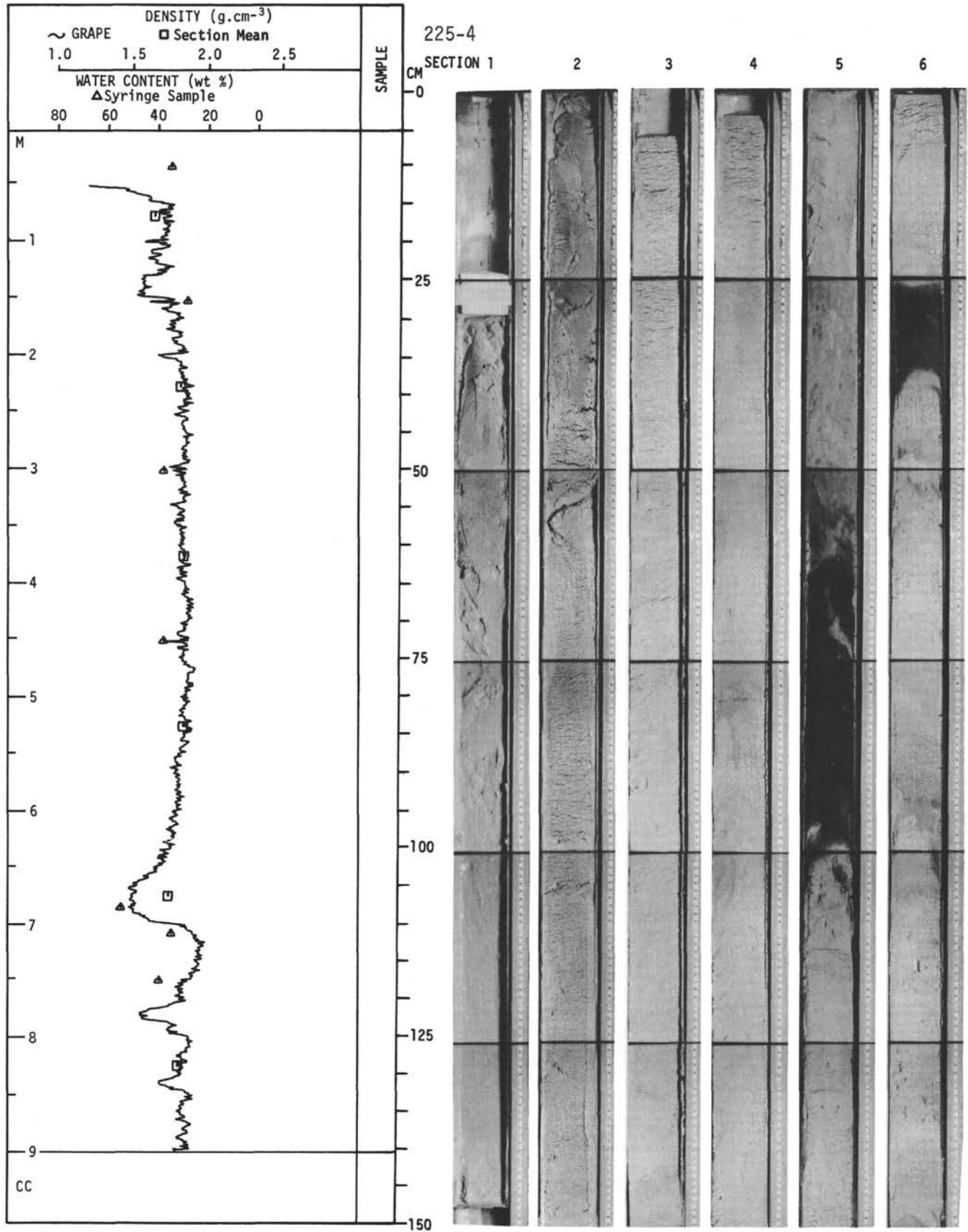
Explanatory notes in chapter 2



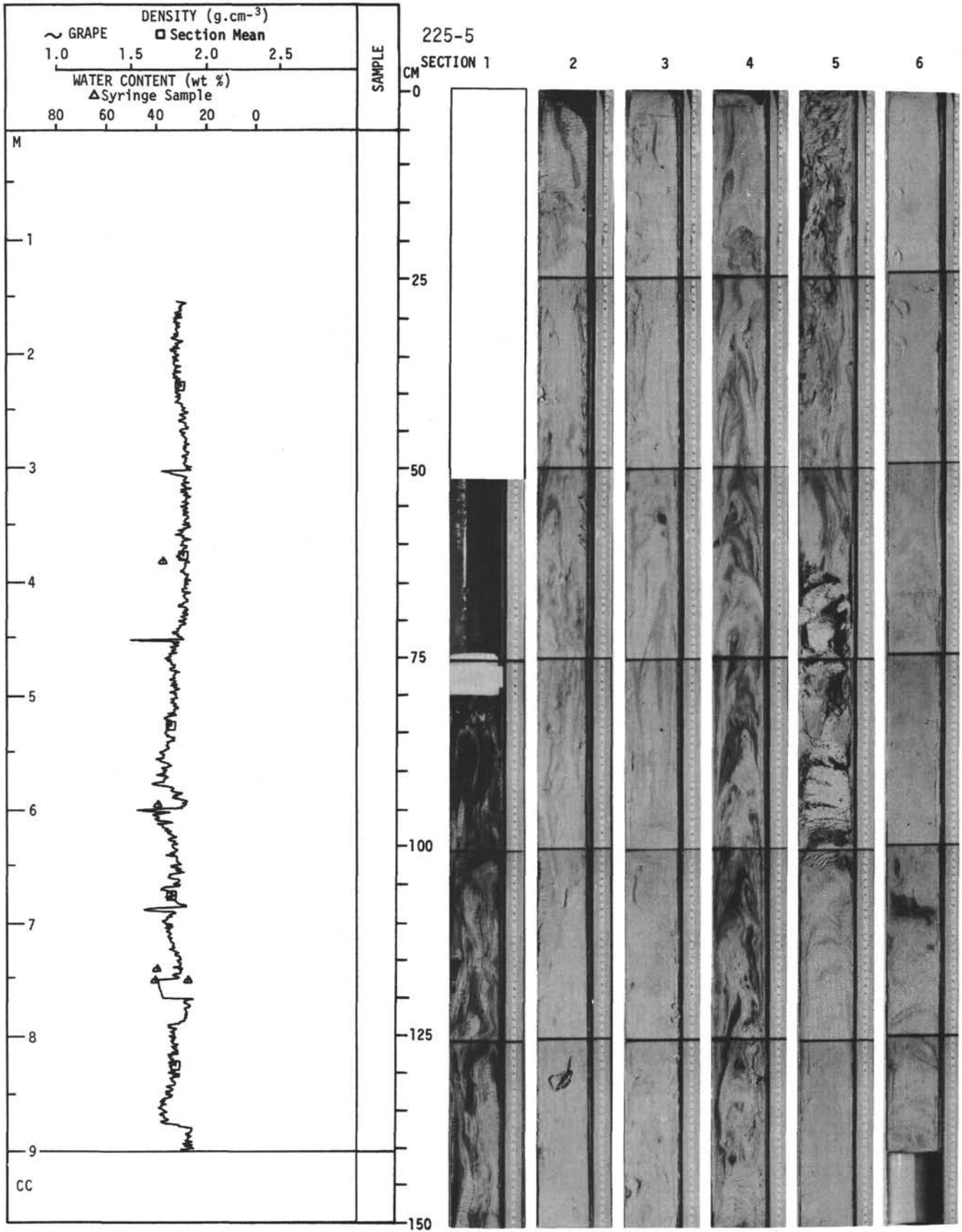
For Explanatory Notes, see Chapter 2



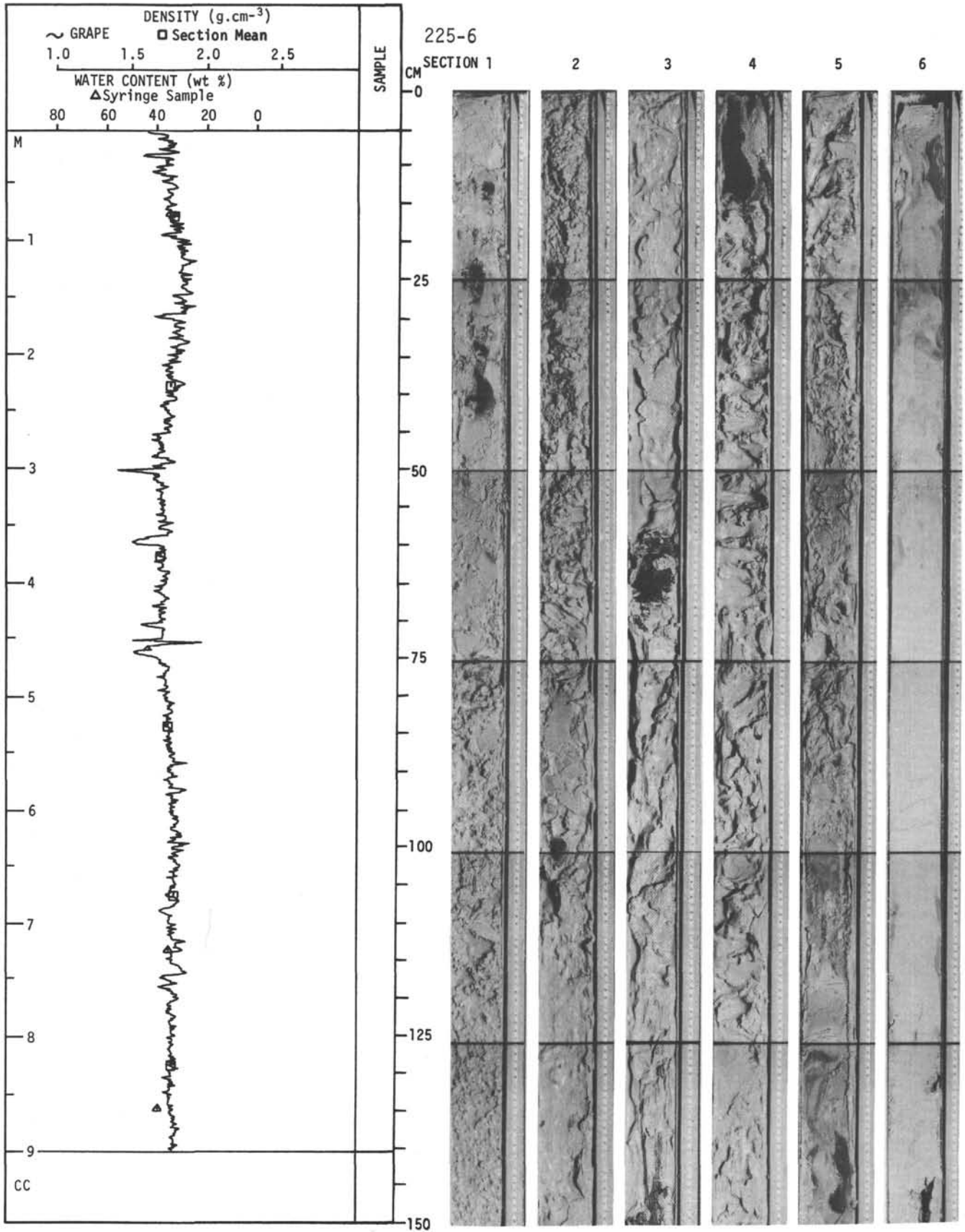
For Explanatory Notes, see Chapter 2



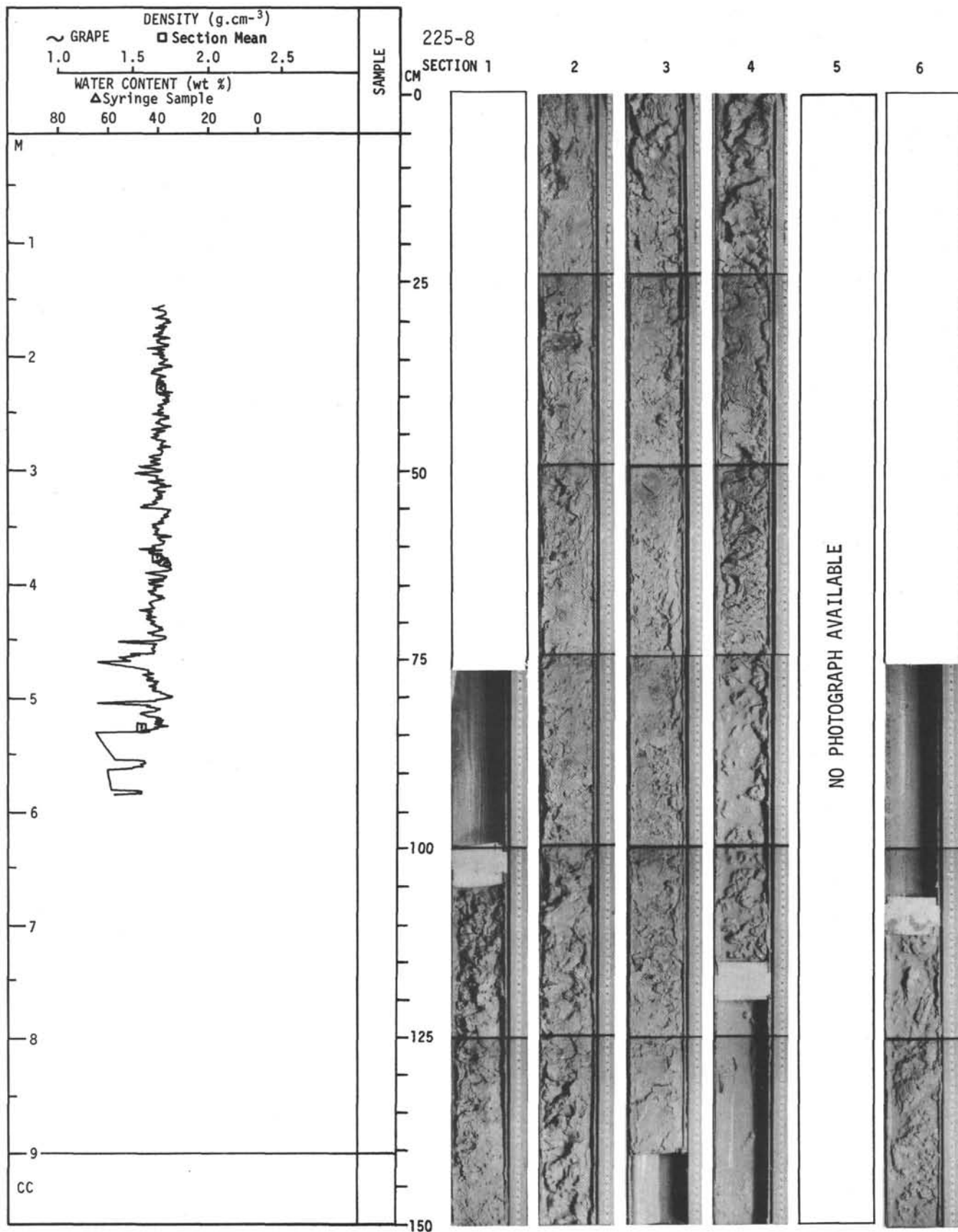
For Explanatory Notes, see Chapter 2



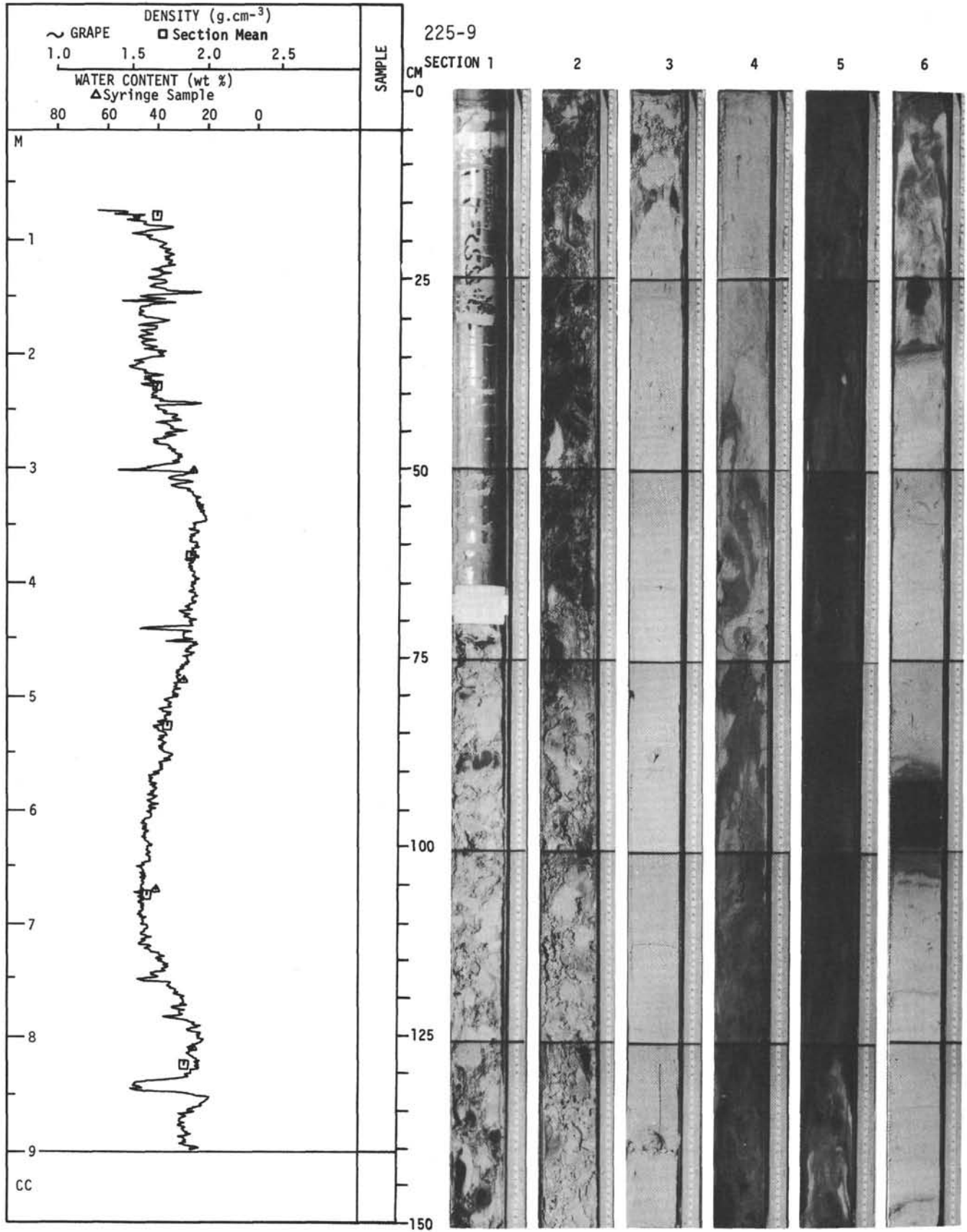
For Explanatory Notes, see Chapter 2



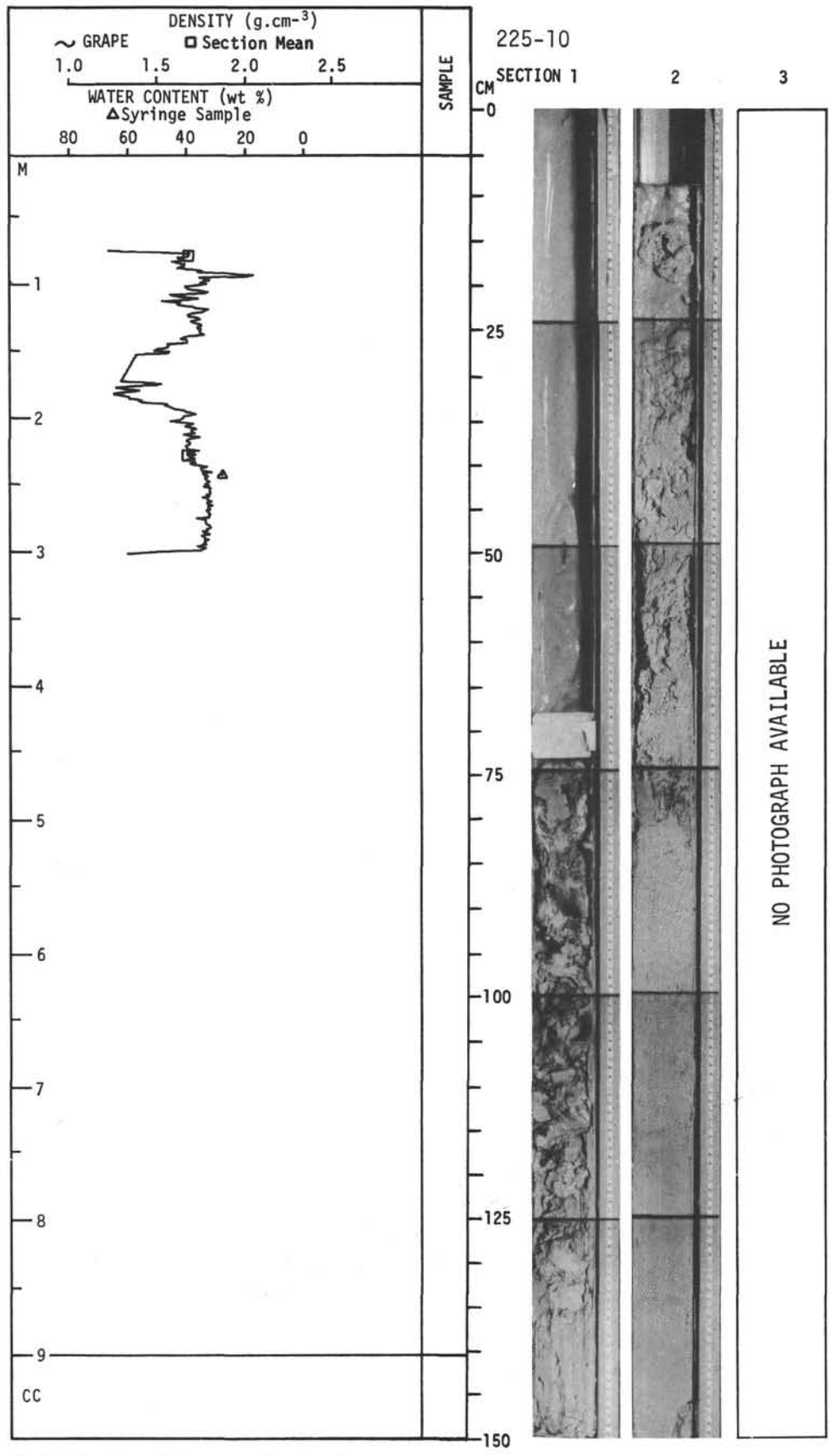
For Explanatory Notes, see Chapter 2



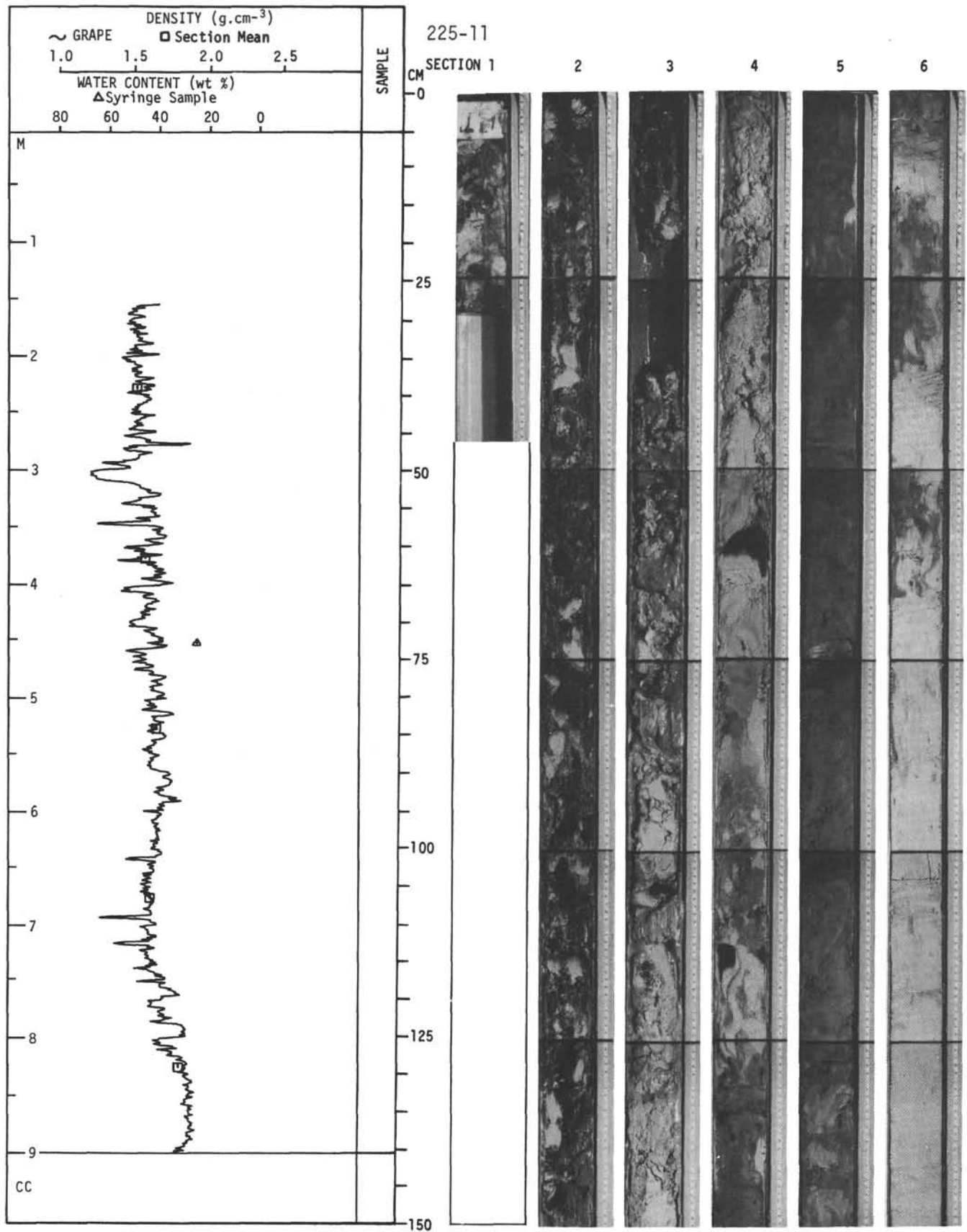
For Explanatory Notes, see Chapter 2



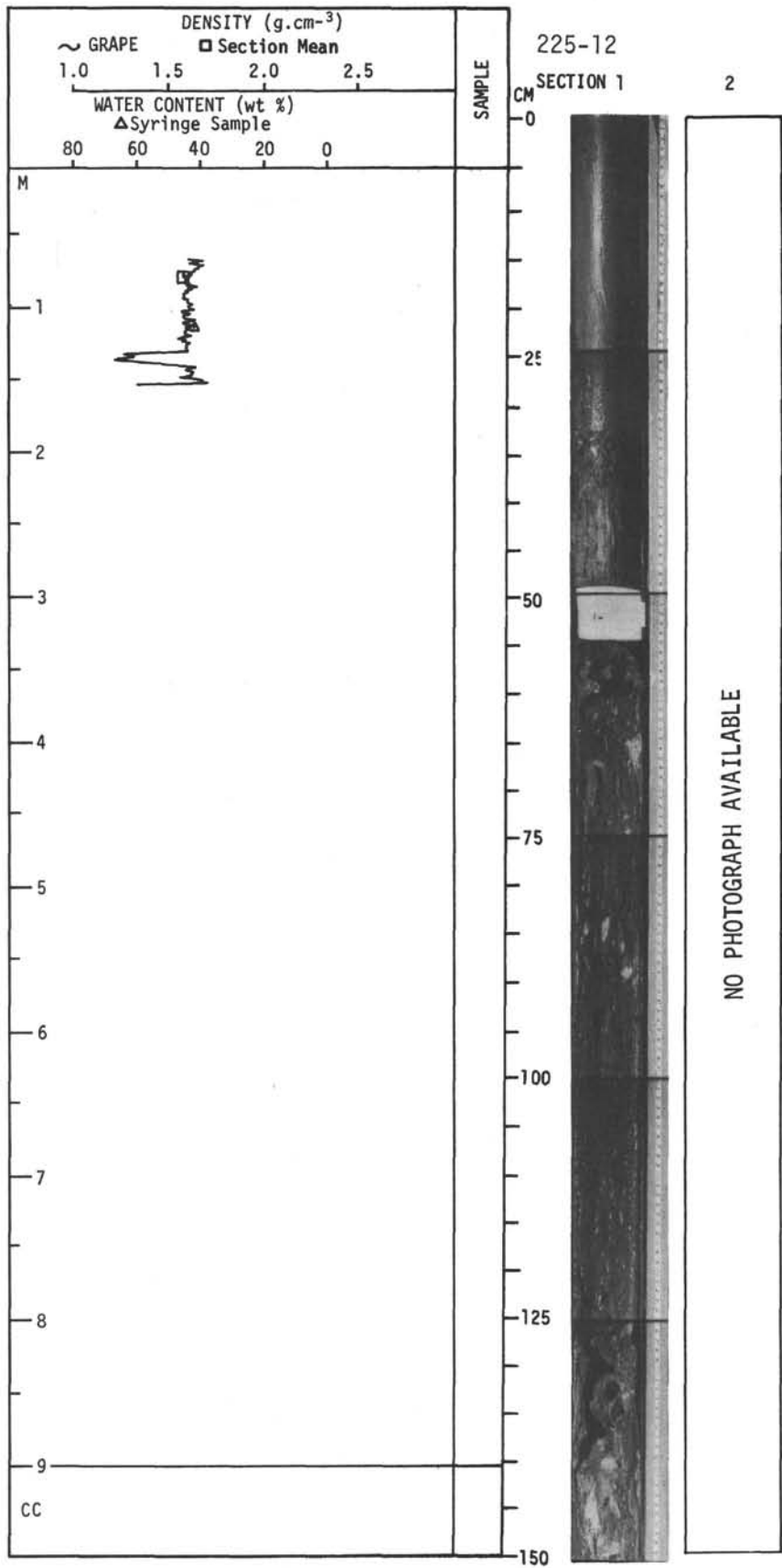
For Explanatory Notes, see Chapter 2



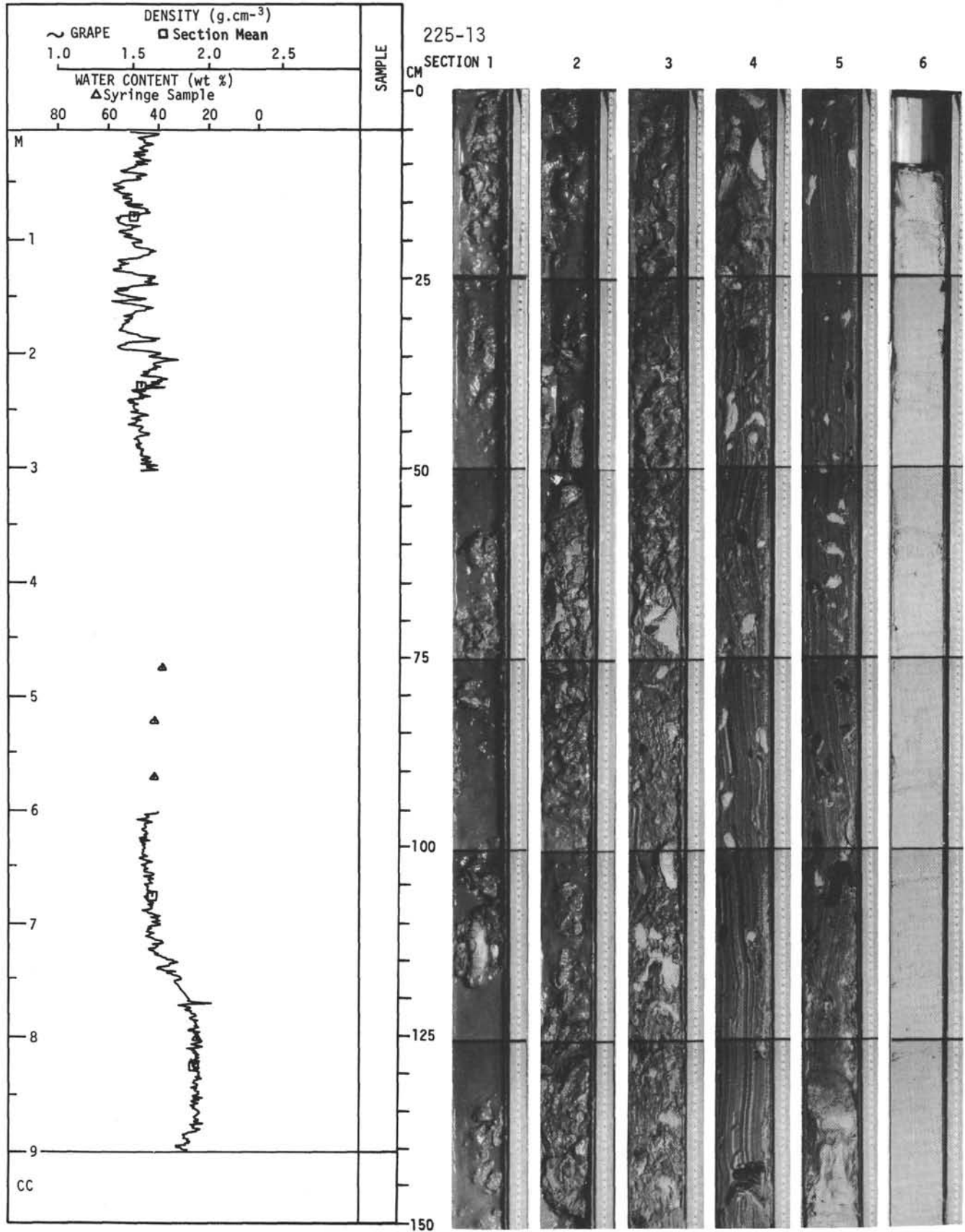
For Explanatory Notes, see Chapter 2



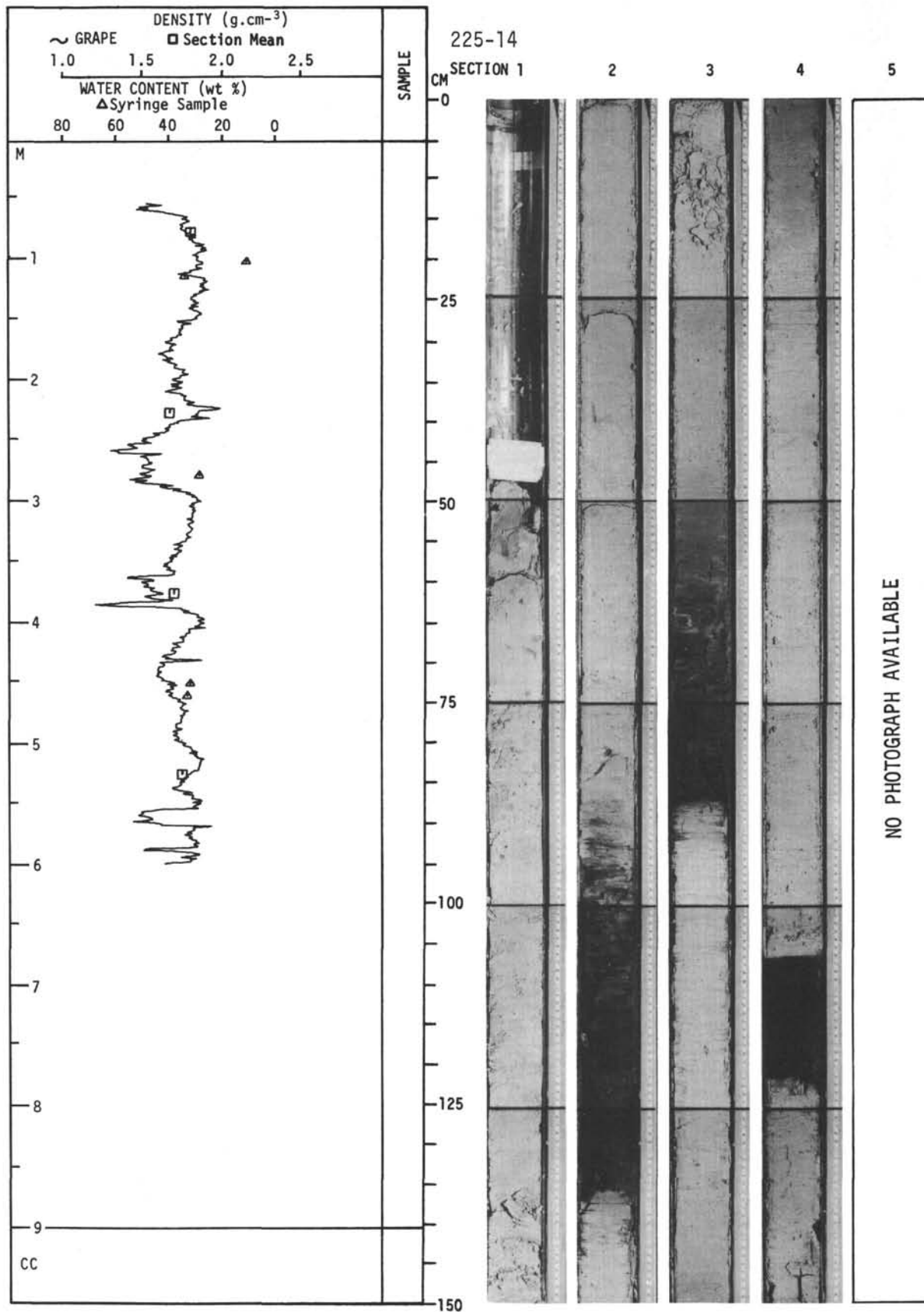
For Explanatory Notes, see Chapter 2



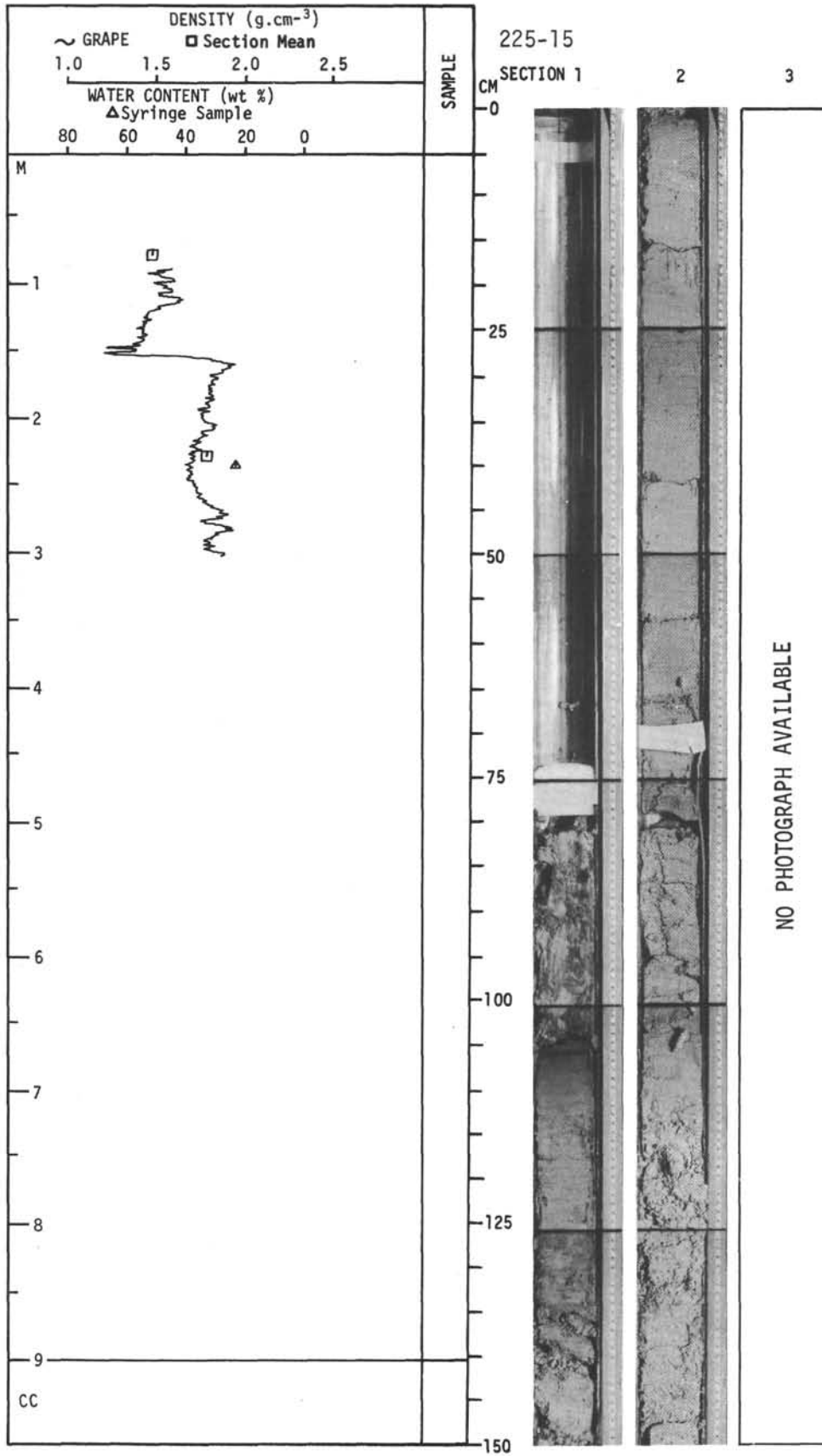
For Explanatory Notes, see Chapter 2



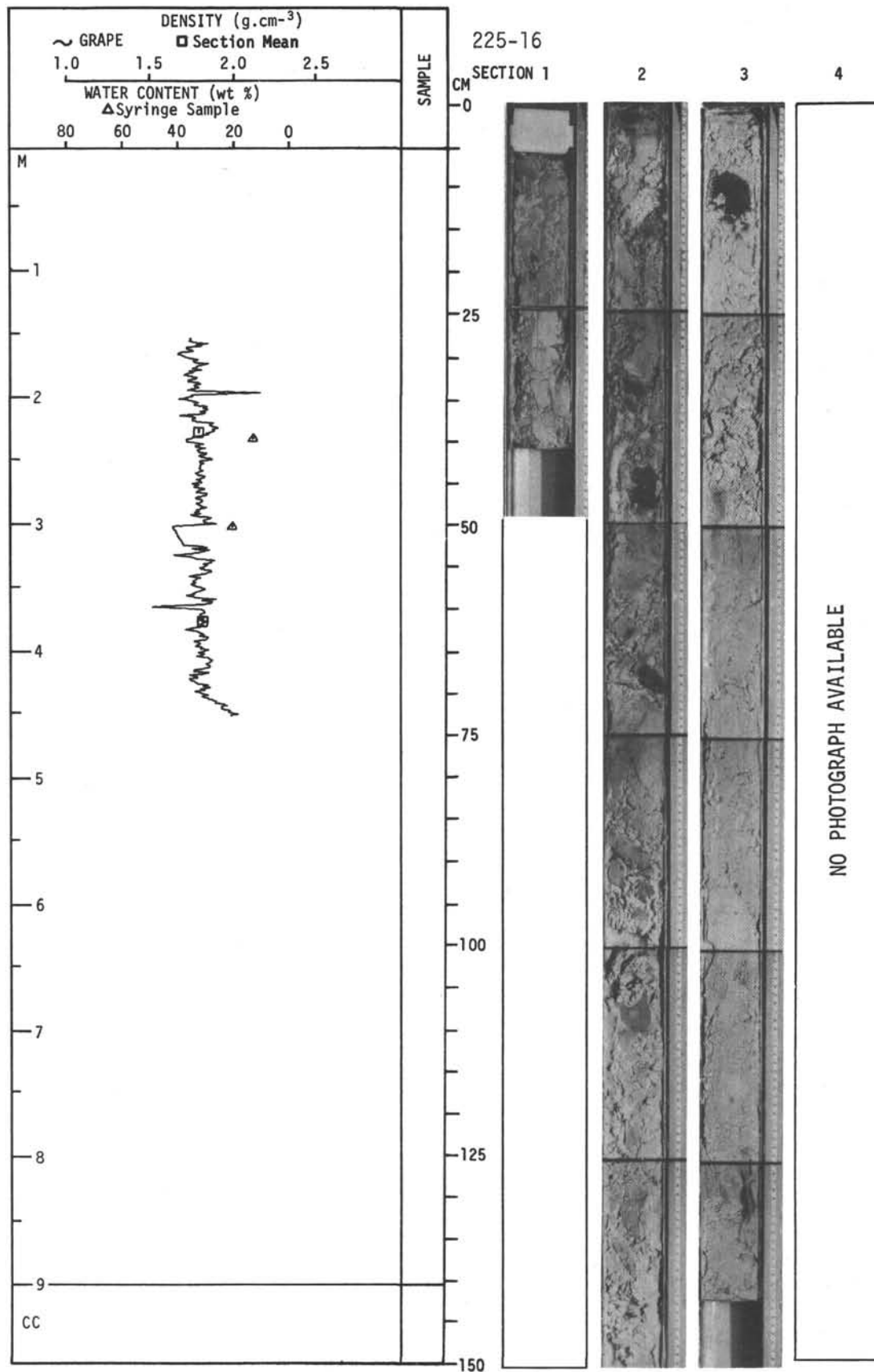
For Explanatory Notes, see Chapter 2



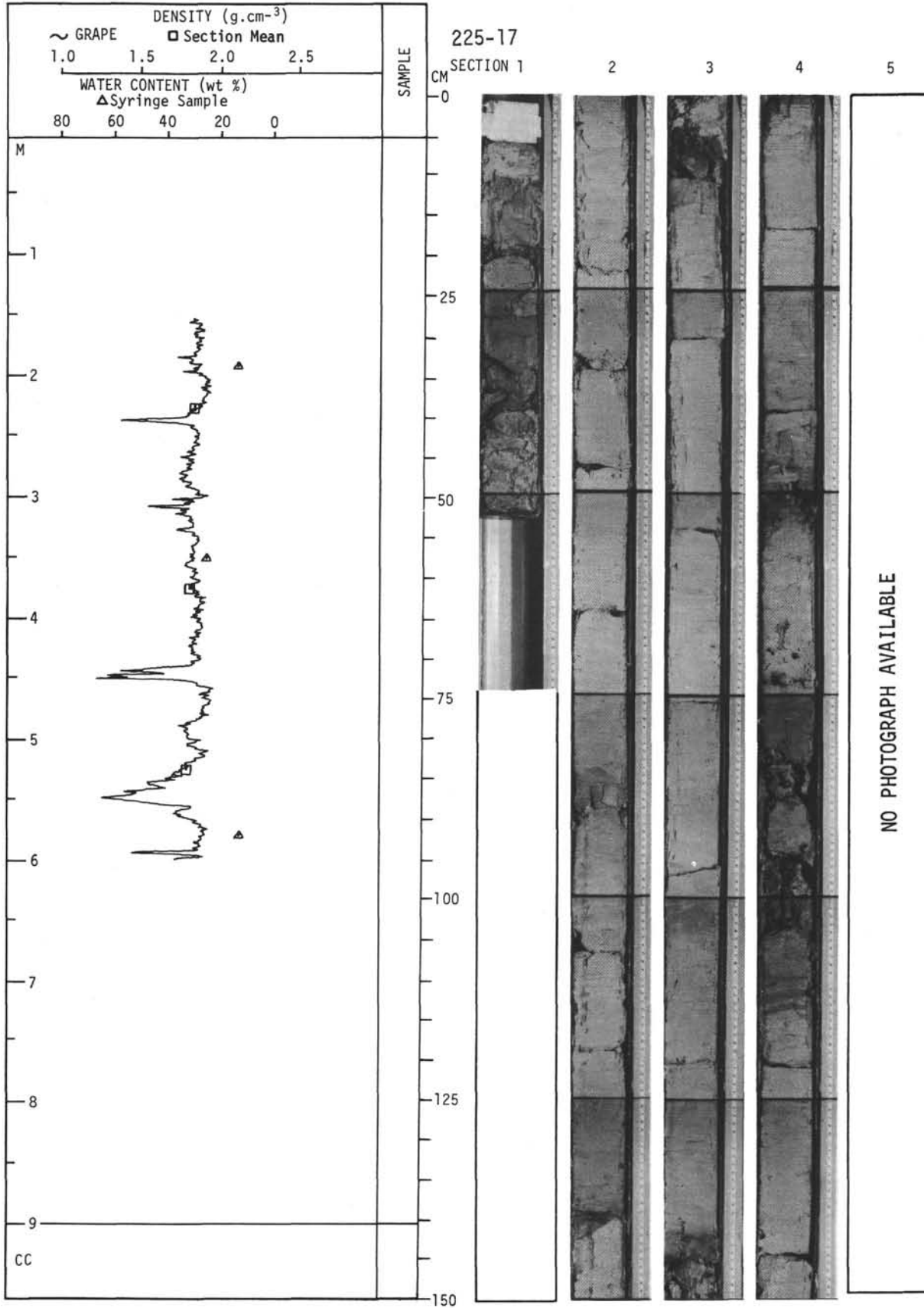
For Explanatory Notes, see Chapter 2



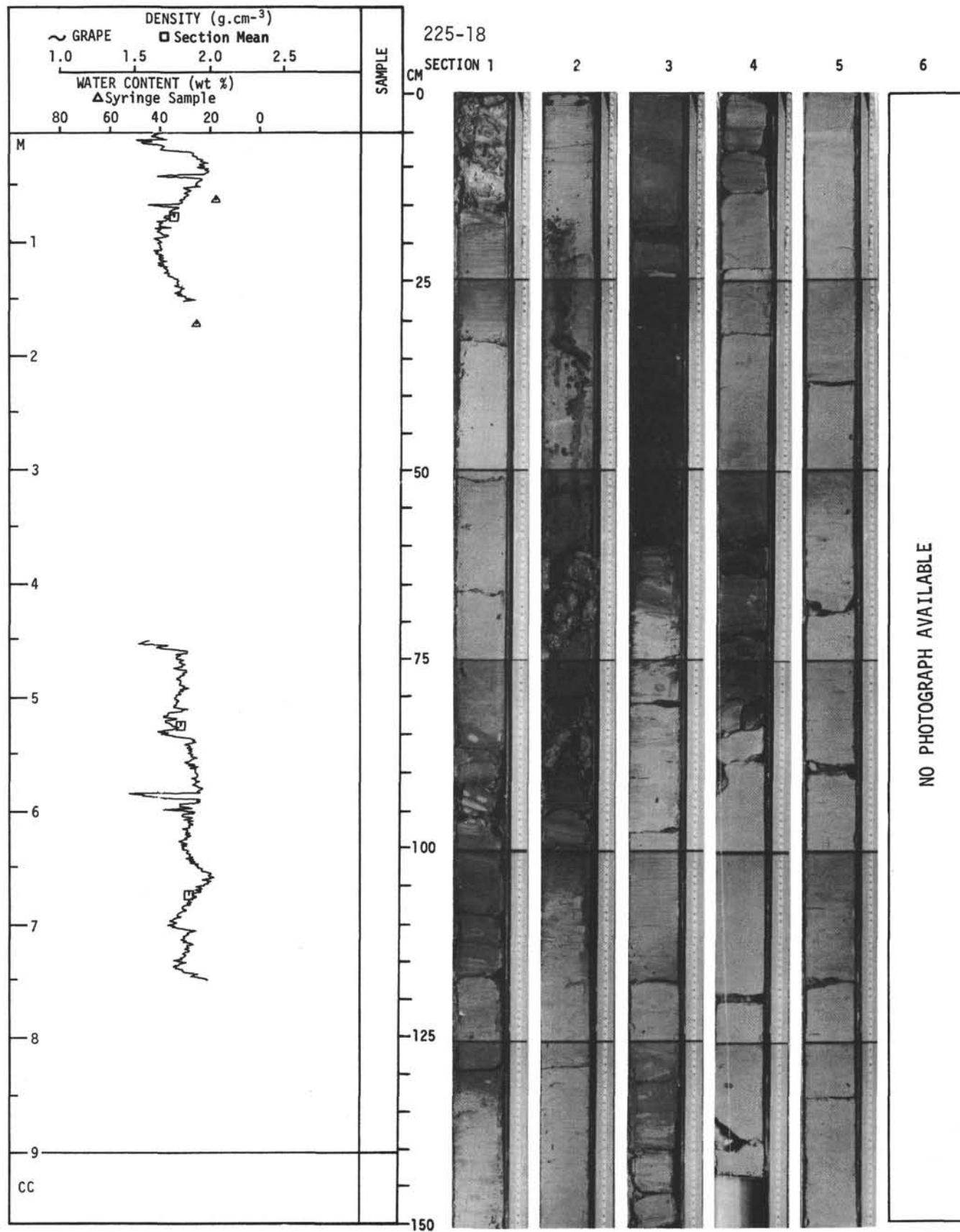
For Explanatory Notes, see Chapter 2



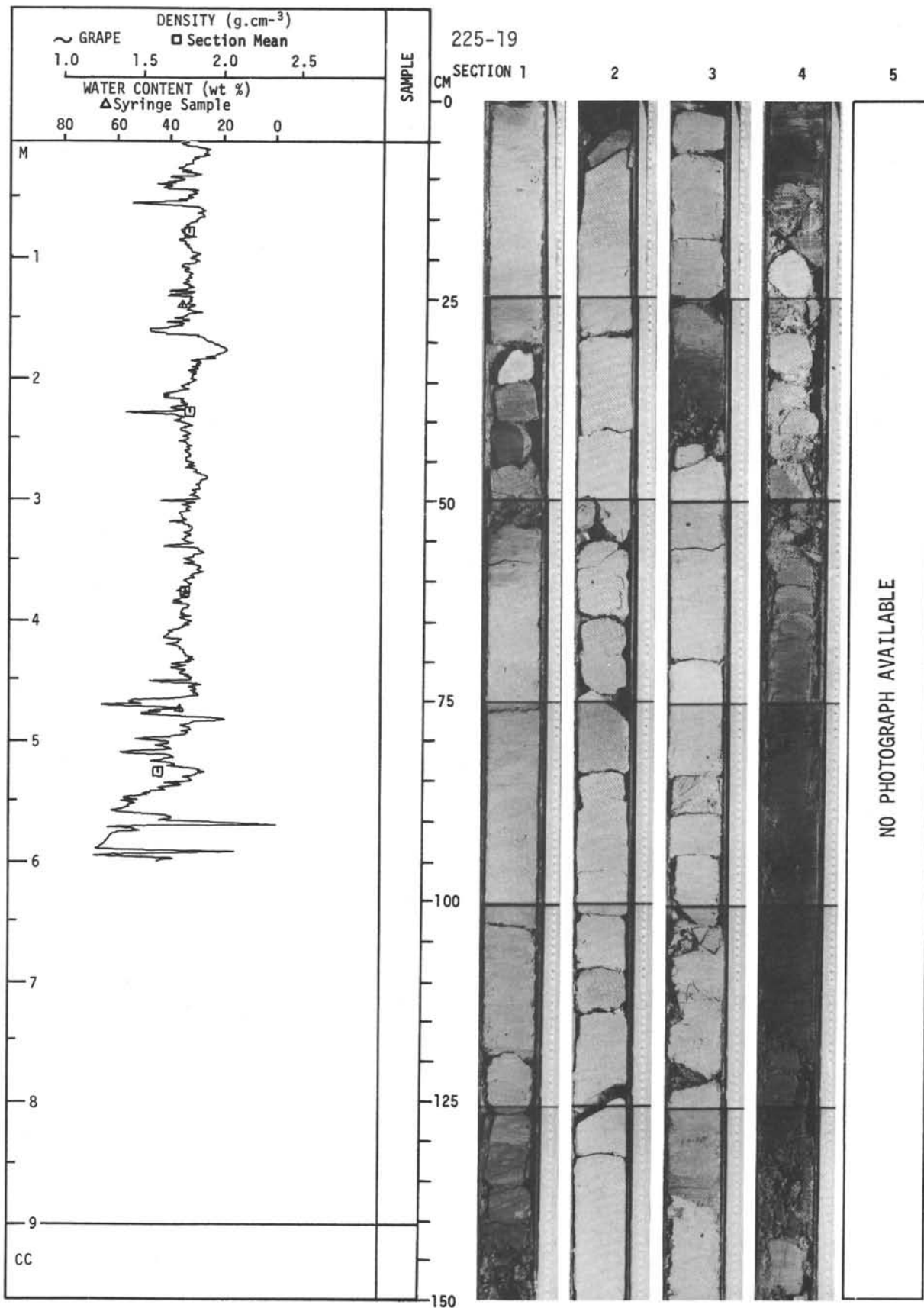
For Explanatory Notes, see Chapter 2



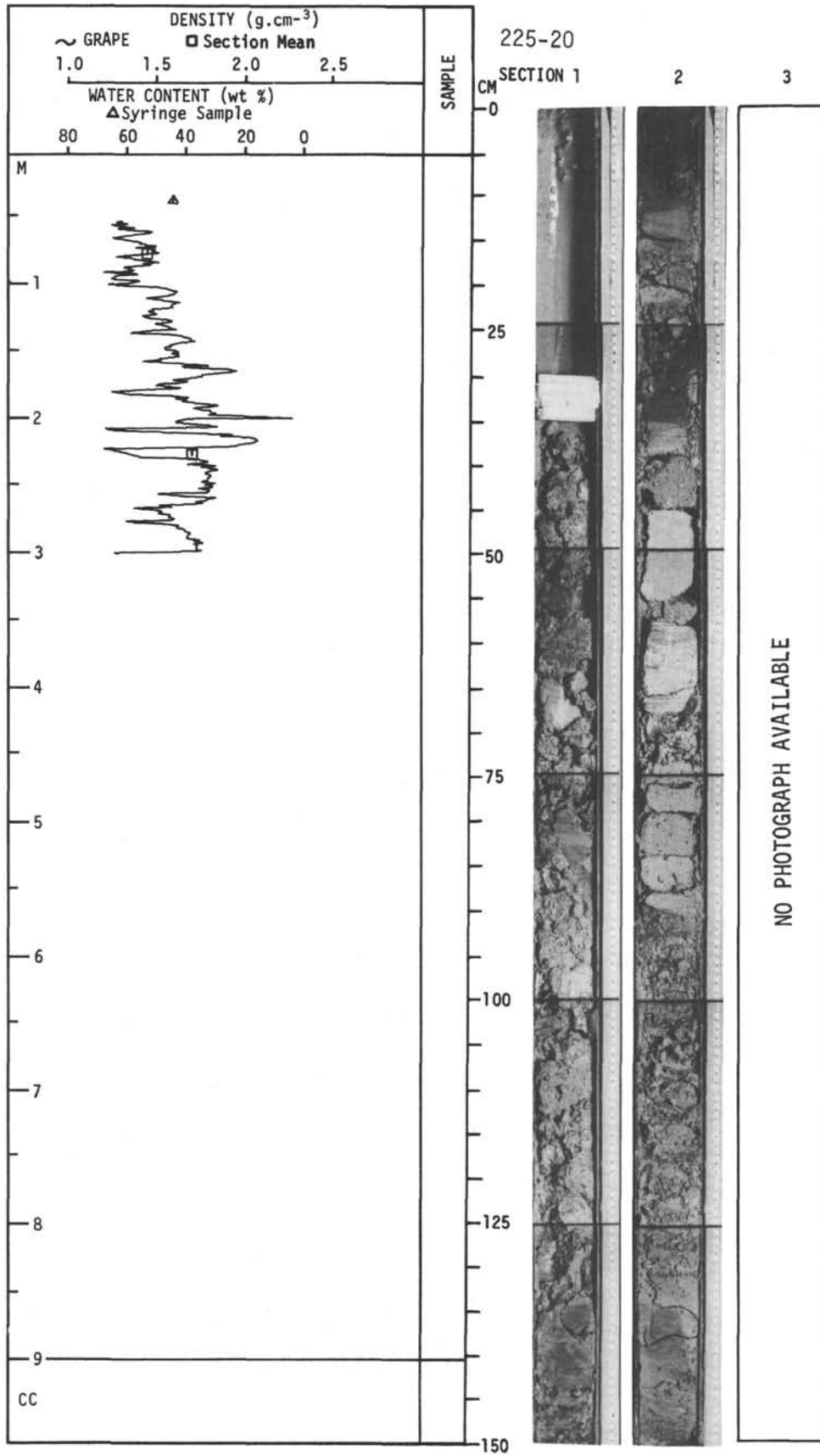
For Explanatory Notes, see Chapter 2



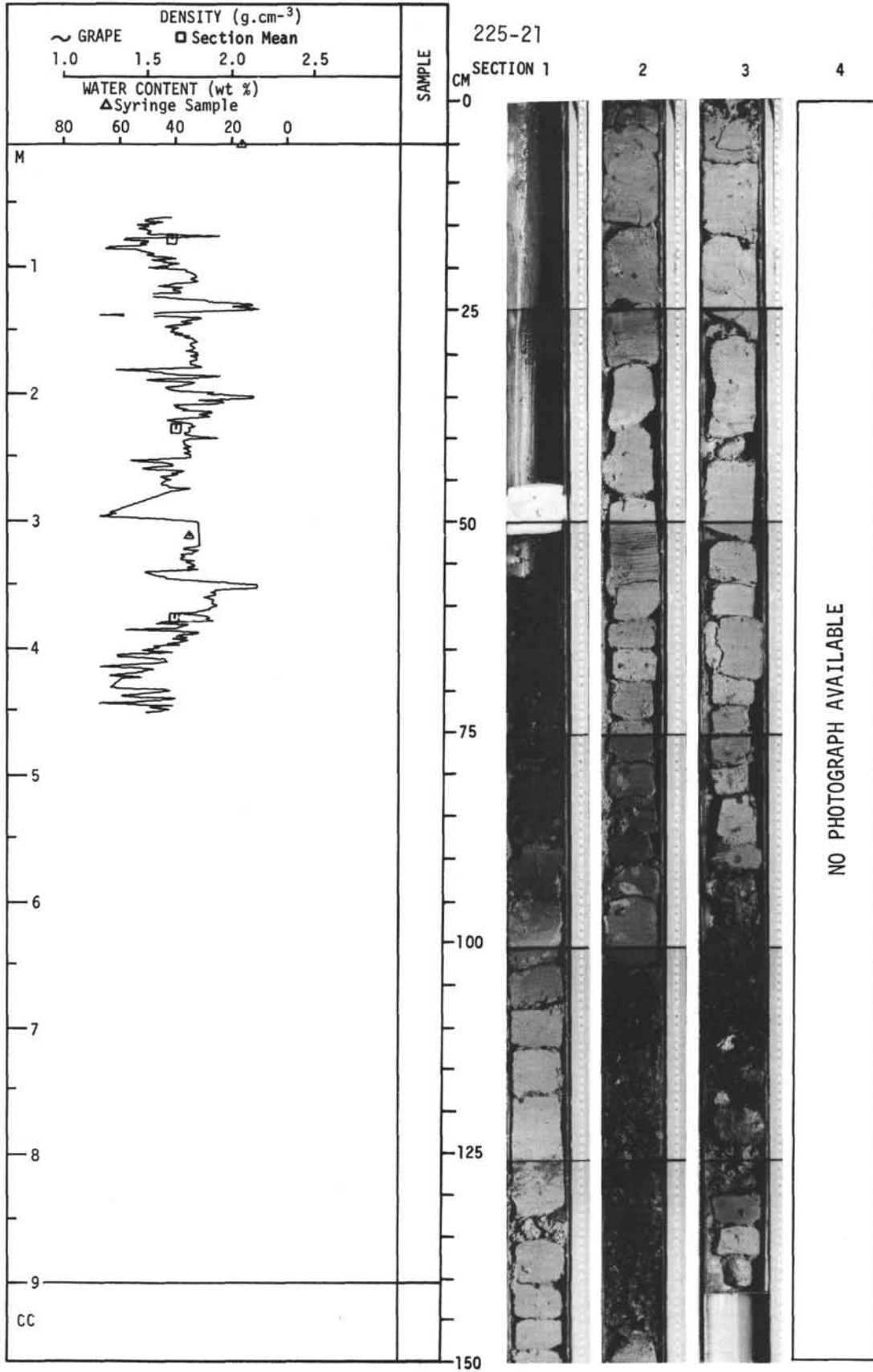
For Explanatory Notes, see Chapter 2



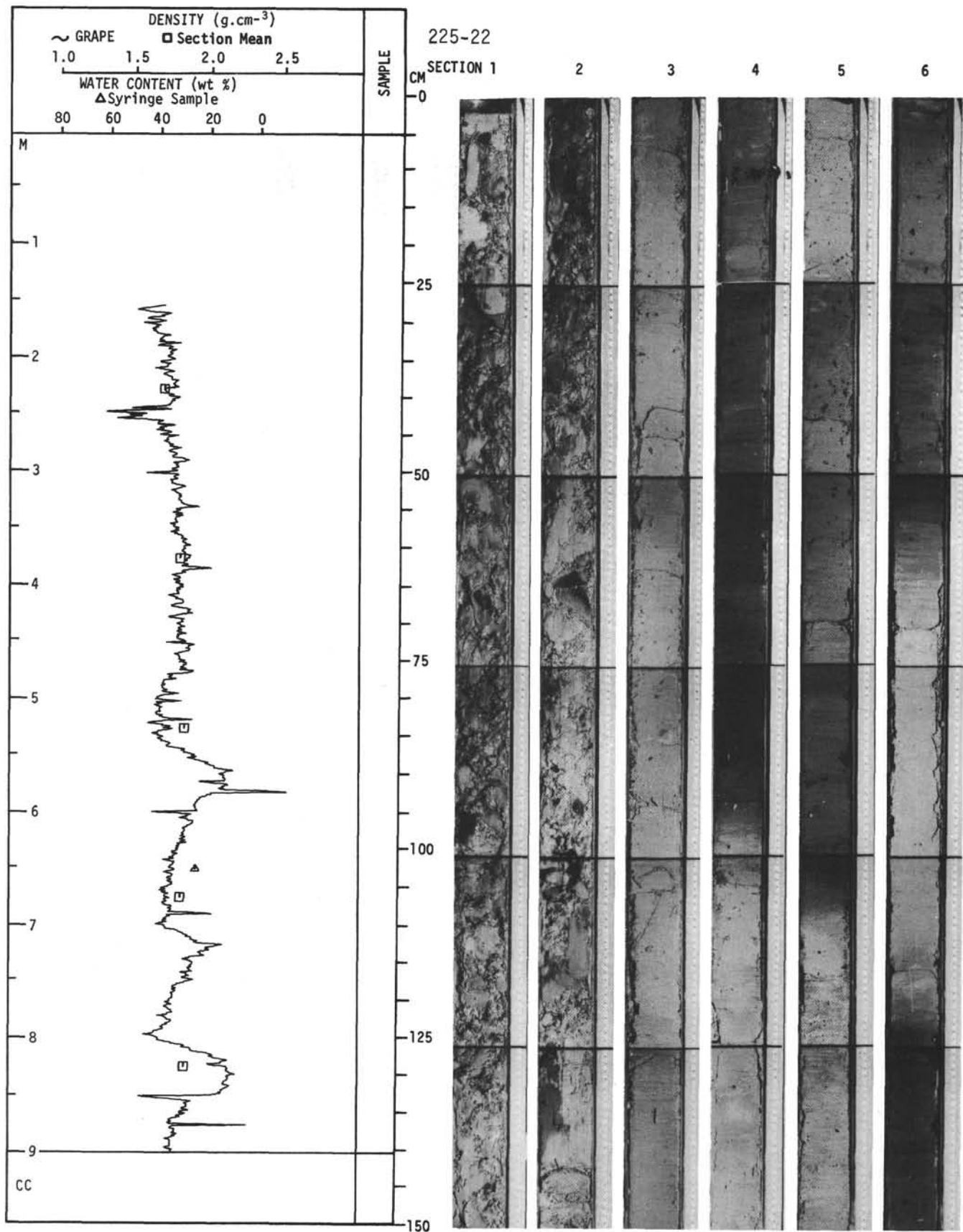
For Explanatory Notes, see Chapter 2



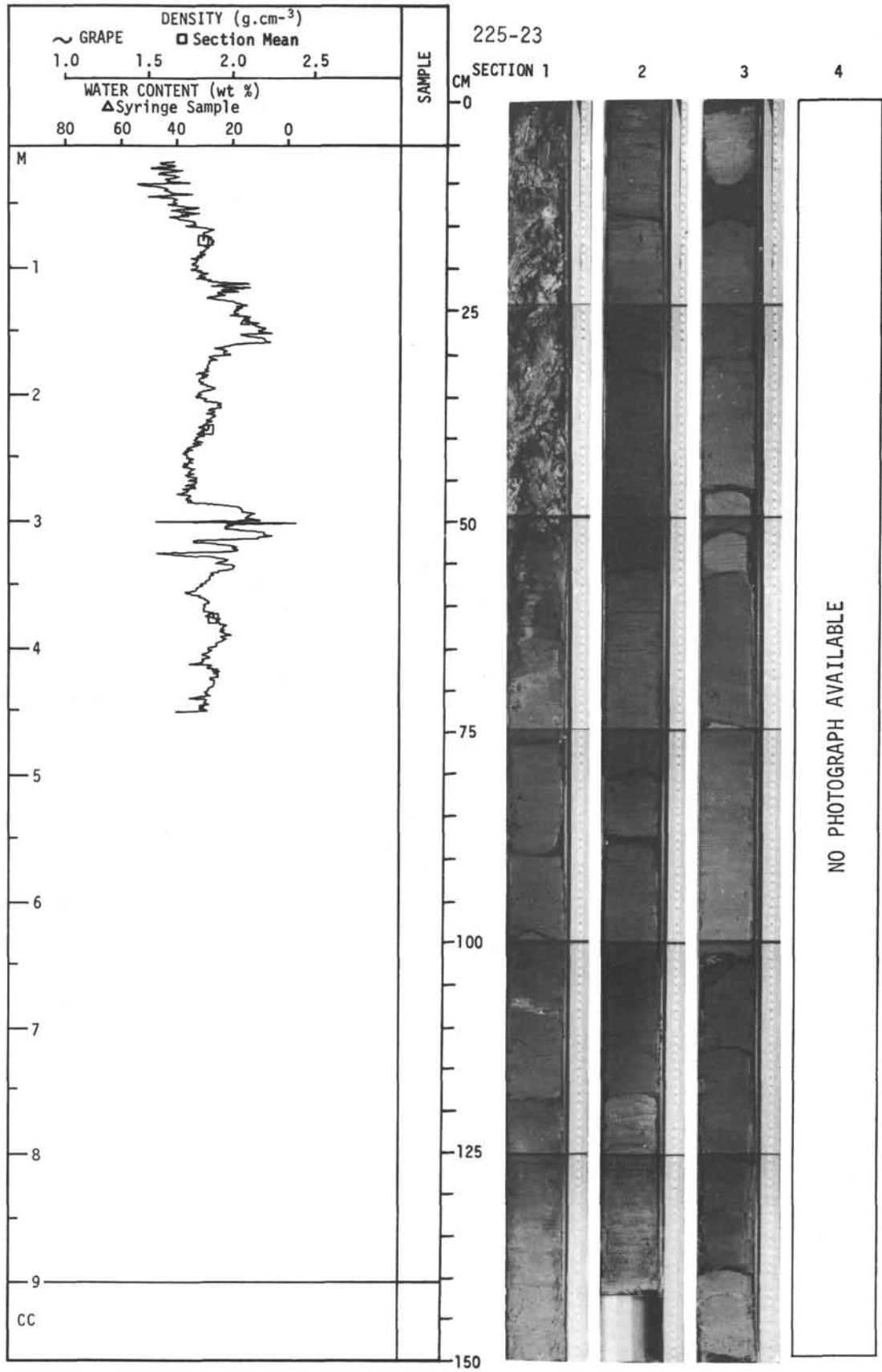
For Explanatory Notes, see Chapter 2



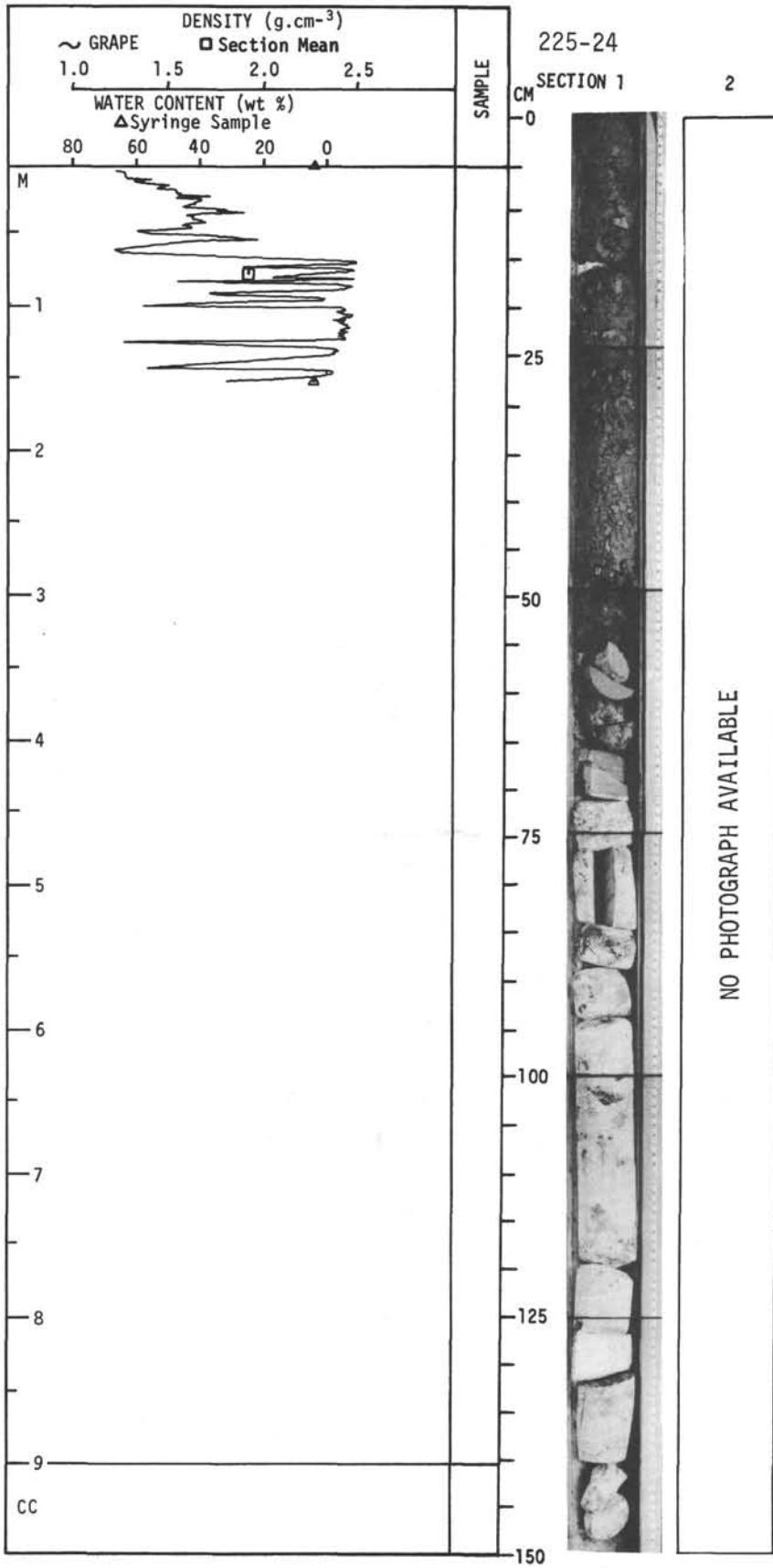
For Explanatory Notes, see Chapter 2



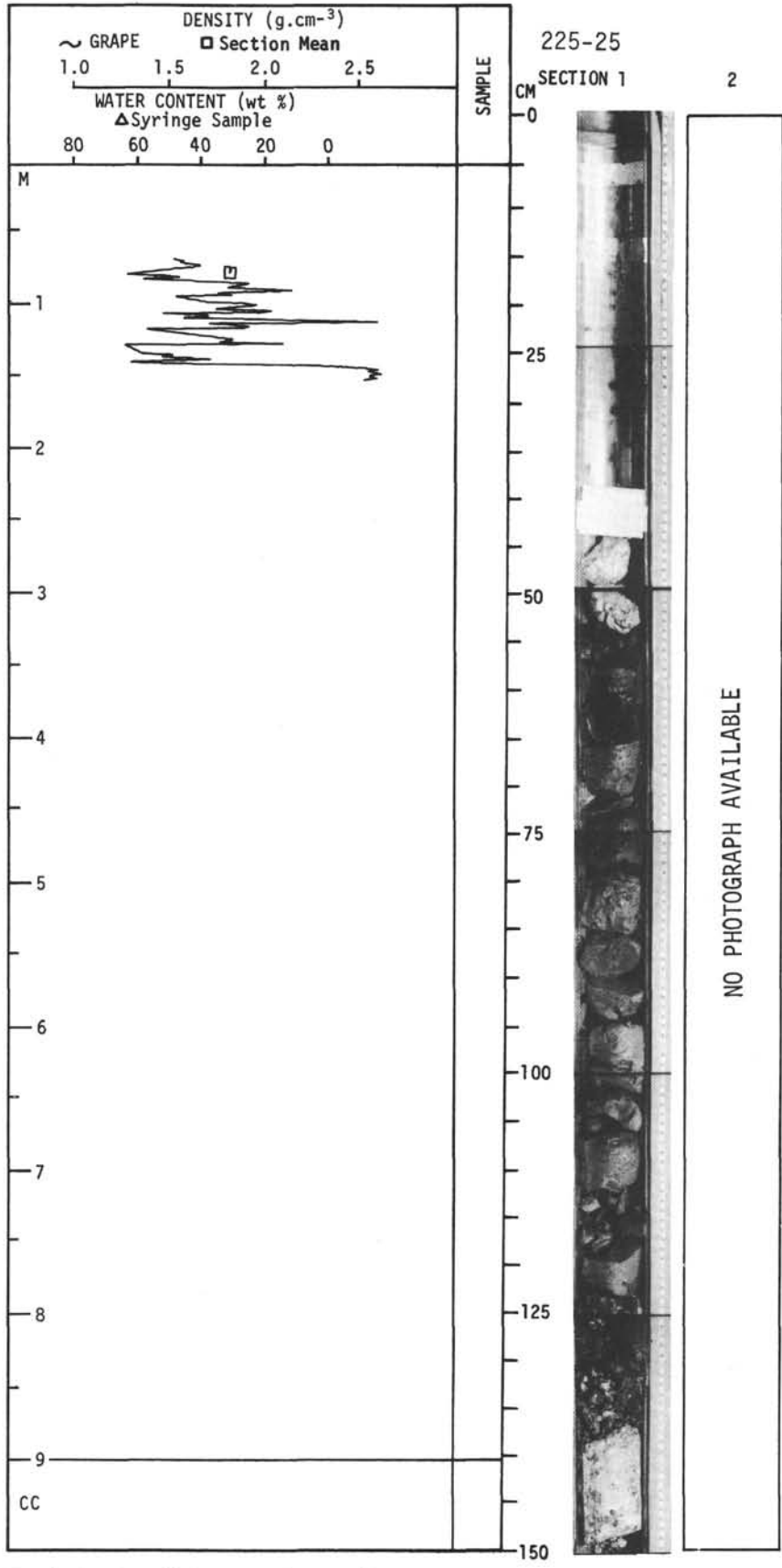
For Explanatory Notes, see Chapter 2



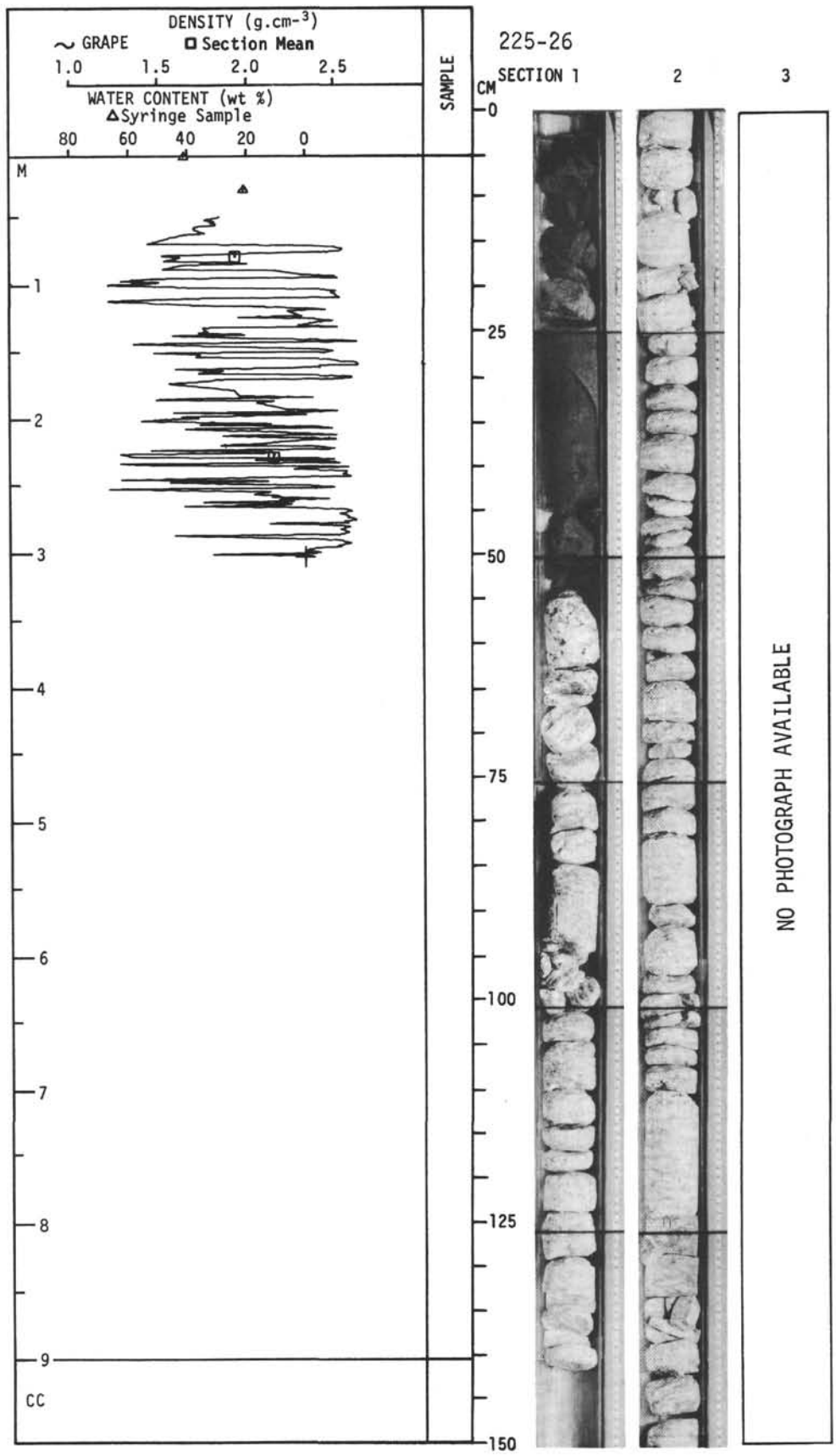
For Explanatory Notes, see Chapter 2



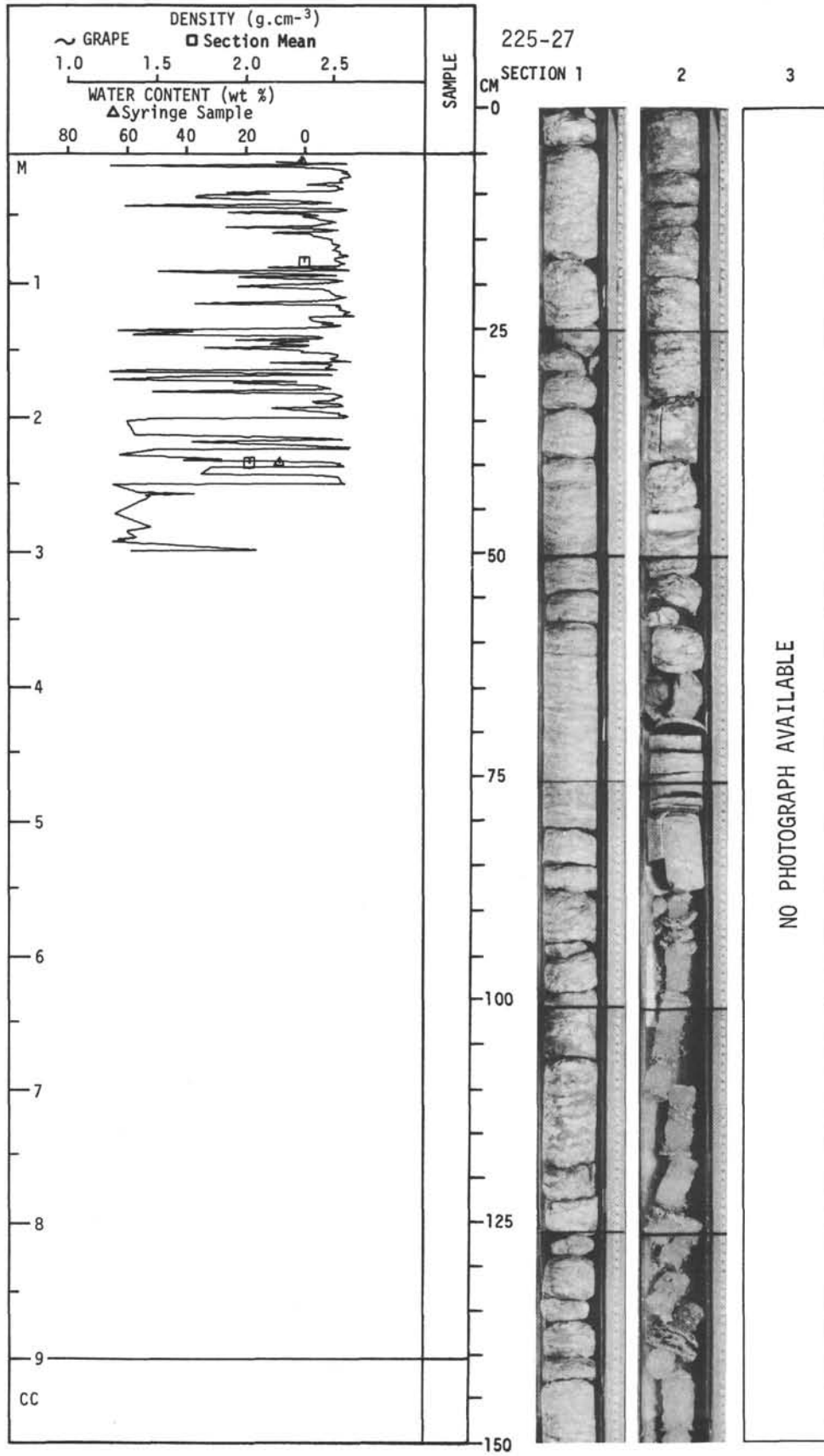
For Explanatory Notes, see Chapter 2



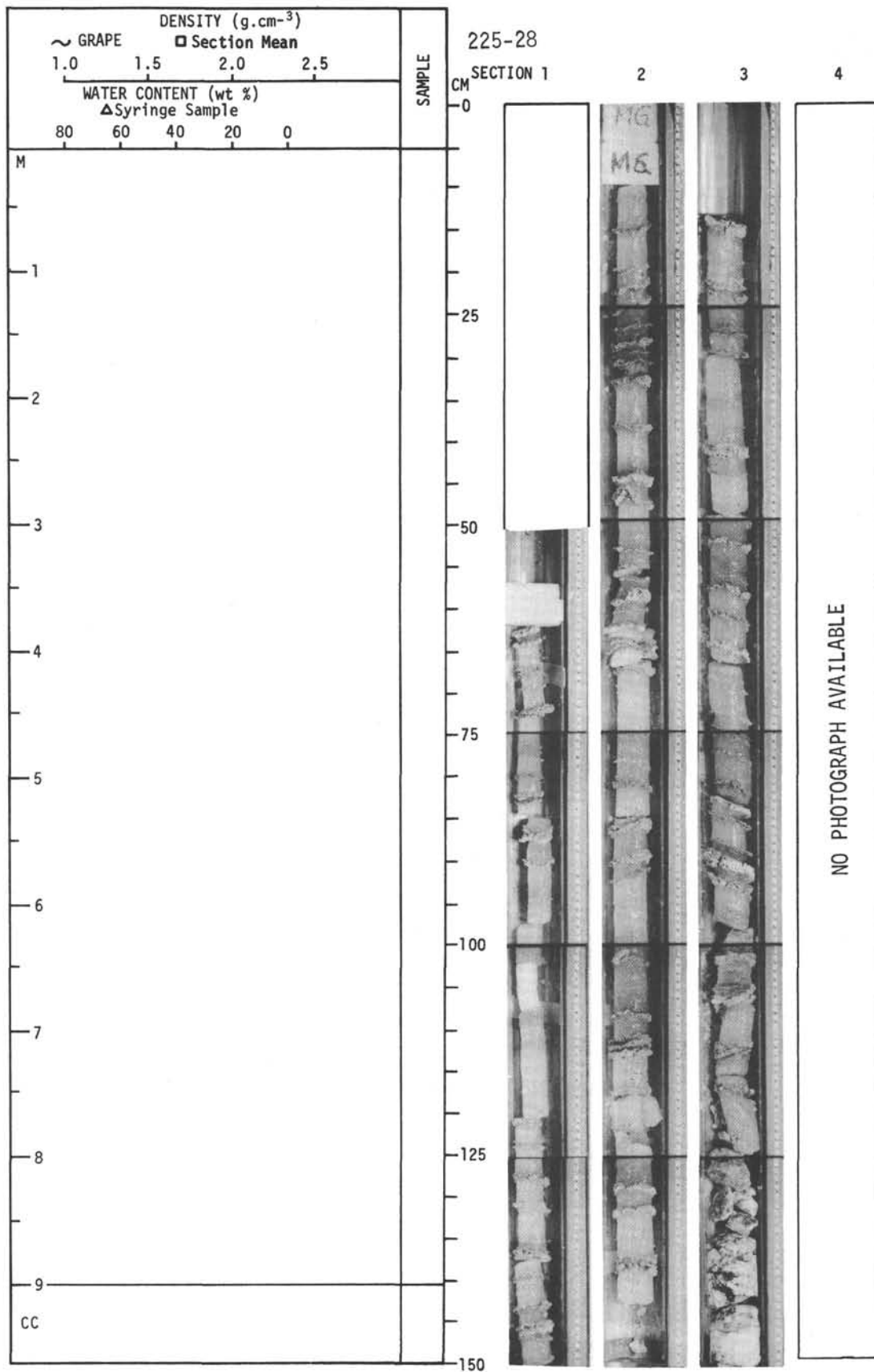
For Explanatory Notes, see Chapter 2



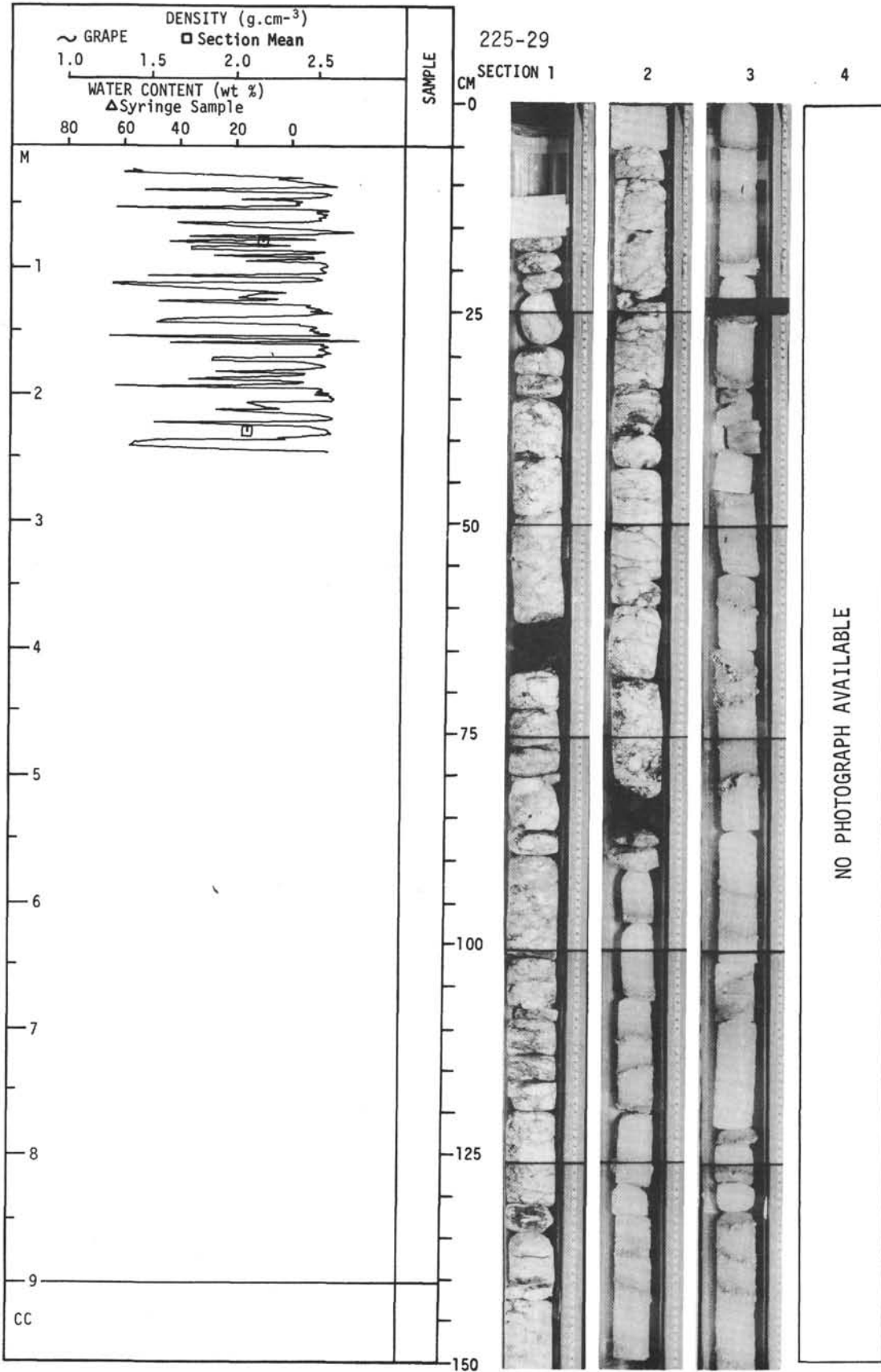
For Explanatory Notes, see Chapter 2



For Explanatory Notes, see Chapter 2



For Explanatory Notes, see Chapter 2



For Explanatory Notes, see Chapter 2